

# **Optimal Synthesis and Design of Advanced Chromatographic Process Concepts**

## **Habilitationsschrift**

von Dr.-Ing. Malte Kaspereit  
geboren am 31. Juli 1973 in Merseburg

zur Verleihung des akademischen Grades

## **Doktor-Ingenieur habitatus (Dr.-Ing. habil.)**

genehmigt von der Fakultät für Verfahrens- und Systemtechnik  
der Otto-von-Guericke Universität Magdeburg am 5. Juli 2011.

Gutachter:

Prof. Dr.-Ing. Achim Kienle  
Institut für Automatisierungstechnik, Otto-von-Guericke Universität Magdeburg

Prof. Dr.-Ing. Andreas Seidel-Morgenstern  
Institut für Verfahrenstechnik, Otto-von-Guericke Universität Magdeburg

Prof. Dr. Marco Mazzotti  
Institut für Verfahrenstechnik, Eidgenössische Technische Hochschule Zürich

# Contents

## Part I – Summary of Main Results

<b>1</b>	<b>Introduction</b>	<b>1</b>
<b>2</b>	<b>Fundamentals</b>	<b>7</b>
2.1	Basic Operating Modes in Chromatography . . . . .	7
2.2	Modeling of Chromatographic Processes . . . . .	8
2.3	Equilibrium Theory of Chromatography . . . . .	11
<b>3</b>	<b>Advanced Operating Modes</b>	<b>23</b>
3.1	Batch Chromatography with Adsorbing Additives . . . . .	23
3.2	Steady-State Recycling Chromatography . . . . .	26
3.2.1	Design and Performance Under Ideal Conditions . . . . .	27
3.2.2	Design and Performance Under Nonideal Conditions . . . . .	28
3.3	Simulated Moving Bed Chromatography . . . . .	29
3.3.1	Design for bi-Langmuir Isotherms . . . . .	29
3.3.2	Design for Limited Purity Requirements . . . . .	34
3.3.3	Gradients of Adsorbing Additives . . . . .	36
3.4	Optimal Column Arrangements . . . . .	38
<b>4</b>	<b>Process Combinations</b>	<b>41</b>
4.1	SSR Chromatography with Solvent Removal . . . . .	41
4.2	Chromatography with Crystallization . . . . .	42
4.3	Chromatography with Isomerization Reactions . . . . .	45
4.4	Optimal Synthesis of Process Combinations . . . . .	48

<b>5 Integrated Reactive Processes</b>	<b>51</b>
5.1 Thermal Effects in Reactive Chromatography . . . . .	51
5.2 Integrated SMB Processes for Isomerization Reactions . . . . .	53
5.2.1 Conceptional Process Development . . . . .	53
5.2.2 Optimization-based Synthesis of SMB Processes . . . . .	55
5.2.3 Design Method for a Developed 3-zone Process . . . . .	56
5.2.4 Experimental Validation of a Developed 3-zone Process . .	63
<b>Concluding Remarks</b>	<b>65</b>
<b>References</b>	<b>67</b>

## **Part II – Enclosed Manuscripts**

<b>List of Enclosed Manuscripts</b>	<b>81</b>
-------------------------------------	-----------

# **Part I**

## **Summary of Main Results**



# Chapter 1

## Introduction

Separation problems occur in basically any (bio)chemical production process that converts some kind of educt or reactant into a product. The isolation of the desired species from the mixtures of components delivered by such processes is one of the fundamental tasks in chemical engineering.

The difficulty of a separation depends on the properties of the involved substances. The problem is the more difficult, the closer the physico-chemical properties of desired and undesired species are to each other. Modern productions of fine chemicals, pharmaceuticals and biotechnological products entail more and more frequently the task of isolating a complex and sometimes “fragile” compound at high purity and yield from a mixture that contains very similar substances. Probably the most extreme example in this context is the separation of the enantiomers of a chiral compound, which is of critical relevance in pharmaceutical applications. These stereoisomers differ solely in the spatial orientation of functional groups, rendering their material properties basically identical.

Preparative or process-scale chromatography is one of the methods of choice when tackling problems like enantioseparations or the biotechnological production of proteins, because here classical separation technologies like distillation or extraction usually fail. Further reasons for the increasing application of preparative chromatography are its capability of achieving very high purity as well as its flexibility. As formulated by Guiochon *et al.* [1, p. 2]: “*No industrial separation technique is more versatile than chromatography, nor better suited for the rapid production of milligram to ton quantities of highly pure products. None has a comparable separation power.*”

Despite the undoubted capabilities and relevance of chromatographic processes, it is a common mindset among chemists and engineers to conceive the technology as “expensive” and “last resort”. This is in part due to the periodic and nonlinear na-

ture of chromatographic processes, which makes their basic design more difficult than that of, for example, a distillation process.

On the other hand, operating and investment costs can be significant in chromatography, considering the required high-purity solvents, sophisticated stationary phases, as well as hardware for chromatographic columns and modern concepts like the simulated moving bed process.

This work is intended as a contribution towards improving the performance and applicability of chromatography as an industrial separation technique by devising advanced process concepts that fully exploit the potential of the technology. Strong focus is furthermore on the development of simple design methods for such concepts in order to foster their practical implementation.

A systematic approach is attempted by pursuing the different general options that exist from a process engineer's perspective for creating advanced processes. The developments are based on suitable mathematical process models which are applied in classical and modern frameworks for process synthesis and design.

The scope of most investigated concepts is on binary separations with a certain emphasis on the production of enantiomers. However, all results are readily applicable to other binary problems and some can be extended also to multi-component separations.

From an engineer's perspective, chromatographic processes have a high degree of freedom. This means that there exist many possible options for enhancing the performance of separations by chromatography. While this makes their optimal design difficult, it supports the expectation that purposeful interventions should lead to significant improvements of process performance.

The many interference options arise from the specific nature of chromatography. The technique exploits differences in the distribution equilibria of solutes between two phases. Consequently its separating capacity can be influenced directly by the choice of these phases and the operating conditions. Chromatography is a spatially distributed process. This suggests introducing also spatially distributed manipulations. Almost all chromatographic processes are operated periodically – incidentally also the “continuous” simulated moving bed technology. In conjunction with the typically nonlinear distribution equilibria, this causes a particular dynamic process behavior which is reflected in the more or less complex spatio-temporal patterns of the internal concentration profiles.

The internal concentration profiles of chromatographic processes can be effectively influenced by the chosen boundary conditions as well as their periodic modu-

lation. This can be exploited to enhance the performance in some of the concepts discussed in this work.

In addition to influencing the chromatographic process itself, also its embedment into the production scheme is of interest. While many works focus only on the local design of a chromatographic separation, a significant optimization potential arises when considering the interaction of chromatography with other processes in a specific production environment. The possibilities range from the simultaneous optimization of chromatography together with all units located upstream or downstream, over introducing recycle streams, up to the purposeful combination with additional separation technologies and/or chemical reactions treated here. Finally, it is well known that process integration is an attractive approach for improving chemical processes [2]. Correspondingly, also the development of reactive chromatographic processes is in the scope of this work.

In batch chromatography it has been recognized early that not only the choice of stationary and mobile phase and the operating conditions – flow rate, temperature, amount and concentration of feed – can be used to control the separation efficiency. Already more than 60 years ago it was suggested to influence directly the adsorption strength of the components by additional eluent components. The first suggestion in this context was the use of strong adsorbing displacers [3], soon followed by the idea of gradient elution [4]. In particular gradient chromatography has since then become a standard tool in analytical and preparative applications. Various types have been proposed, for example, gradients of solvent strength, pH value, salts, or temperature. A related and increasingly relevant variant is supercritical fluid chromatography (SFC) [5]. An interesting extension of the gradient concept are also the gradients of the stationary phase proposed recently [6]. The vast variety of practical and theoretical works in gradient chromatography cannot be described here. Overviews can be found in, for example, [7, 8].

Due to its rather simple process setup, only few structural modifications of batch chromatography were investigated. Most important to mention is the implementation of recycle streams. There exists a number of concepts that recycle a partially resolved elution profile over a column to enhance the quality of separation, namely closed-loop recycling (CLR) [9–11], CLR with peak shaving [10] and steady-state recycling (SSR) in mixed-recycle [12] or closed-loop [13] mode, respectively. More details on SSR chromatography will be given in Section 3.2. Another option for a structural modification that inherits potential for performance improvement is to distribute the stationary phase within an optimized arrangement of a number of (identical) columns [14], [PII-6]. Finally, also many reactive chromatographic separations were investigated for single-column processes, see *e.g.* [15–23].

The use of gradients has naturally also been suggested for SMB processes. Besides temperature gradients [24–27], which are difficult to implement in practice, in particular solvent gradients were implemented successfully [28–32]. Gradients of the pH value [33] and salt concentration [34–37] play an increasing role in bioseparations. Also supercritical fluids were applied [38–43].

The more complex setup of SMB processes offers more options for structural modifications than in batch chromatography. An interesting idea that purposefully exploits the nonlinear adsorption behavior is the enrichment and partial recycling of the extract stream [44, 45] (“enriched extract”, EE-SMB). Many investigations aim at extending applicability of the SMB technology to the separation of more than two components. Corresponding concepts for multi-component separations have been proposed. A natural choice is to apply cascades of SMB units [46, 47]. In other approaches side streams and more zones are used to separate three or more fractions [48–51], [52, 53] (“three-fraction”, 3F-SMB).

The periodic nature of the SMB process has inspired various improved operating modes that are based on a dynamic variation of operating parameters. In a conventional SMB unit all operating parameters are held constant throughout operation. A “super-periodic” manipulation of one or more of them can enhance performance. The first reported example is to vary flow rates during the switching interval [54–56] (denoted as “PowerFeed”). Later, an asymmetric switching was proposed that results in a variable column configuration [57, 58] (“VariCol”). Also the feed concentration can be modulated [59–61] (“ModiCon”). Some of these concepts were compared in optimization studies [62, 63]. In another class of operating modes certain internal or external streams are turned on and off in sub-intervals between two switching events, for example, the feed stream [64, 65] (“Partial feed”). More generally, the performance can be enhanced by alternating internal recycling and product withdrawal intervals [66–68] (“Intermittent” operation, I-SMB). A related suggestion is to discharge some product [69] (“Partial discard”). The resulting decreasing yield can be circumvented by fractionating the product and installing a non-permanent recycle [70–72] (“Fractionation & feedback”, FF-SMB). Concepts that realize a variable configuration by turning on and off streams were also developed for multi-fraction separations [73, 74].

The idea of performing chemical reactions in SMB units has attracted considerable interest. While Hashimoto’s concept with side reactors [75] is conceived in the context of this work as a *partially* integrated process, many studies are devoted to analysis and application of *fully* integrated countercurrent and simulated moving bed systems that utilize chromatographic reactors, see *e.g.* [76–86].

The different advanced operating modes for SMB processes have been summarized in several reviews [87–90]. One is included in Part II of this work [PII-1].

Performance Improvement		
<b>Operating modes</b> <ul style="list-style-type: none"><li>• Gradients: additives, modifiers, ...</li><li>• Recycling techniques</li><li>• Super-periodic operation</li></ul>	<b>Process combinations</b> (Flowsheet level) <ul style="list-style-type: none"><li>• Combined separations</li><li>• Combined separation and reaction</li></ul>	<b>Integrated processes</b> (Apparatus level) <ul style="list-style-type: none"><li>• Reactive separations</li><li>• Hybrid separations</li></ul>

**Figure 1.1** – General approaches for the development of improved processes in preparative chromatography.

It appears useful to classify the various options for developing improved chromatographic processes that were discussed above. From a process engineering perspective the classification shown in Figure 1.1 is suggested. The concepts investigated in this work can be grouped into the three categories shown.

These three classes were also applied to structure this work. After a review of the theoretical fundamentals in Chapter 2, different *Operating modes* are investigated in Chapter 3, *Process combinations* are discussed in Chapter 4, and *Integrated processes* are developed in Chapter 5.



# Chapter 2

## Fundamentals

### 2.1 Basic Operating Modes in Chromatography

All processes and concepts to be discussed in this work are based on two fundamental chromatographic operating modes. These are the conventional single-column or batch chromatography, and the (semi-)continuous simulated moving bed process. Below the basic operating principles of both modes will be recapitulated briefly. More detailed explanations can be found in the standard literature, for example, in [1, 91].

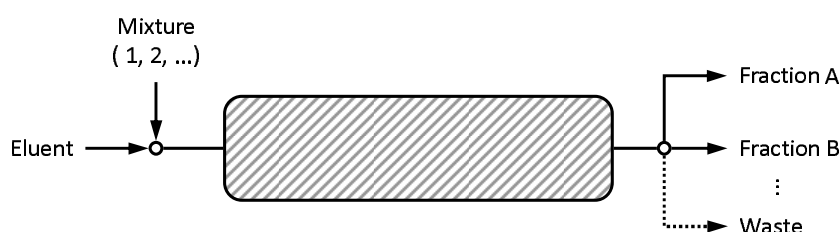


**Figure 2.1** – Basic scheme of batch chromatography.

Single column or batch chromatography as illustrated in Fig. 2.1 is the most widely applied chromatographic operating mode. In the elution mode that is considered in this work, a finite volume of a mixture containing components 1, 2, etc. is injected into a continuous stream of eluent. Due to differences in their thermodynamic distribution equilibria, the solutes migrate at different velocities through the bed. The resulting elution bands are collected at the column's outlet in the product fractions *A*, *B*, etc.

Specific advantages of batch chromatography are its capability of separating multi-component mixtures with very similar properties, a rather fast method development, and its high versatility [1]. On the other hand, drawbacks are its discontinuous feed supply and its limited performance in terms of solvent consumption

and productivity, in particular when considering binary separations.

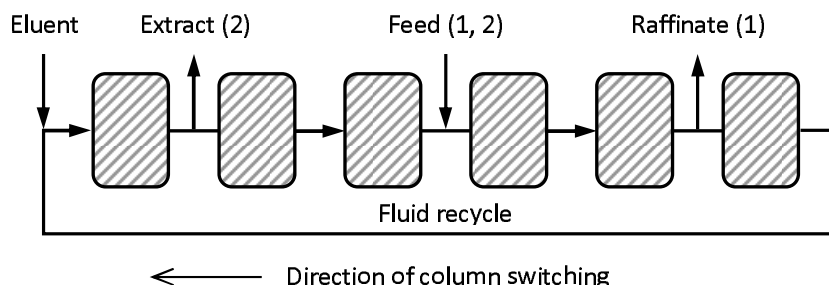


**Figure 2.2** – Basic scheme of simulated moving bed (SMB) chromatography.

A sophisticated alternative to batch chromatography is the simulated moving bed (SMB) technology [92]. As illustrated in Fig. 2.2, this concept creates a counter-current between the fluid and solid phases by periodically switching the columns against the direction of the fluid flow. A conventional SMB process separates a continuous feed stream into two fractions. The weaker retained species is obtained in the raffinate port, while the stronger retained elutes with the extract stream. More details on the principles of SMB chromatography and improved operating concepts can be found in several reviews [88, 89, 93], [PII-1].

Obviously the classical SMB concept in Fig. 2.2 is particularly suited for binary problems. In fact, it became a standard technique for enantioseparations. Due to its countercurrent nature, it achieves a high driving force for the separation. Thereby a significantly lower solvent consumption is achieved in comparison to batch chromatography and, depending on the process configuration, often also a higher productivity.

## 2.2 Modeling of Chromatographic Processes

Designing a preparative chromatographic process typically requires an appropriate mathematical process model that can predict the elution profiles of the components with sufficient accuracy. In general the modeling task is not trivial due to the periodic nature and nonlinear dynamics of chromatography, but also due to the different dispersive effects that are responsible for band broadening. A considerable number of different models and modeling approaches exists. Below only a brief summary on the topic can be given. Extensive discussions on the derivation of the different models, proper initial and boundary conditions for the different process concepts, their (numerical) solution as well as comparisons and possible classifications can be found in, for example, in [1, 91, 94–97].

The core of any chromatographic process model is constituted by the mass balances for the individual components within a single column. In this context, the minimum requirement is to account for the convective transport of the solutes and to apply an expression for their distribution equilibria. Energy balances are less frequently used because preparative application is mainly restricted to liquid chromatography, where the heat effects due to the typically weak interactions can be neglected. The momentum balance is mostly replaced by some simple correlation for the pressure drop.

The following simplifying assumptions are commonly made in the derivation of the mass balance equations [91]:

- Homogeneously bed packed with uniform spherical particles,
- Constant density and viscosity of the mobile phase,
- Isothermal operation,
- Negligible radial distributions.

Apart from these simplifications, a number of dispersive effects can occur in a chromatographic column:

- Axial dispersion due to molecular and eddy diffusion between the particles,
- External mass transfer from the bulk to the particle boundary layer,
- Diffusion in the pores of the particles,
- Diffusion on the surface of the particles,
- Kinetics of adsorption and desorption onto the surface.

Various models have been proposed that differ with respect to the consideration and possible simplification of these dispersive effects. Table 2.1 gives an overview of those that are applied most frequently. Note that the table represents rather an ordered list than a strict classification. The models are arranged in the order of decreasing complexity and a subdivision is made according to the number of effects used to describe band broadening.

The choice of an appropriate model for a particular application depends on the dominating dispersive effect(s) and the required level of accuracy. Detailed models like the general rate model require significant experimental efforts for their parameterization and suffer from slow numerical solutions. Their use can be required in “difficult” applications where large molecules like proteins are separated on macroporous resins. In most practical cases it is sufficient to consider besides axial dispersion a kinetic effect that accounts in a “lumped” manner for all remaining contributions, like in the transport-dispersive and the reaction-dispersive

**Table 2.1** – Overview on common chromatographic models. The asterisk (\*) marks models that assume established adsorption equilibrium.

<b>Band broadening due to ...</b>	<b>Dispersive effect(s)</b>	<b>Model name</b>
... three and more contributions	Axial dispersion External mass transfer Intraparticle diffusion (Adsorption kinetics)	General rate model
	Axial dispersion External mass transfer Internal mass transfer (Adsorption kinetics)	Lumped pore diffusion model
... two contributions	Axial dispersion Overall mass transfer	Transport-dispersive model
	Axial dispersion Adsorption kinetics	Reaction-dispersive model
...single contribution	Adsorption kinetics	Reaction or Thomas model
	Overall mass transfer	Transport model
	Apparent dispersion	Equilibrium-dispersive model *
	Number of CSTRs	Equilibrium-stage model *
	Number of cells	Craig model *
No band broadening	–	Ideal or equilibrium model *

model, respectively. In many cases, in particular for “small molecules” and columns with high efficiency, even a single parameter is sufficient to describe band broadening. Particularly interesting in this context is the equilibrium dispersive model, for which the so-called Rouchon algorithm [98] yields very fast numerical solutions [1, 96].

A separate class in Table 2.1 are the two stage models below the dashed line. These are not based on continuous mass balances. The well-known equilibrium stage model by Martin and Synge [99] assumes a cascade of equilibrium stages which are continuously passed by the mobile phase. It is – at least for linear systems and sufficient column efficiency – analogous to the equilibrium-dispersive model. An exceptional approach is represented by the Craig model [100], which is based on a discrete number of equilibration steps.

The last entry in Table 2.1 is the ideal or equilibrium model of chromatography. It considers only convection and thermodynamics by assuming established adsorption equilibrium. Any dispersive effects are neglected. This limits its applicability for the detailed design in practical applications. However, its simplicity facilitates analytical solutions for many practically relevant applications. Therefore, the model is of great importance for the fundamental analysis of chromatographic processes and the derivation of simple design methods. Due to its relevance for this work, the ideal model will be discussed in more detail in Section 2.3.

## 2.3 Equilibrium Theory of Chromatography

A systematic development of new process concepts requires suitable tools for process analysis and design. The detailed models in Section 2.2 take into account not only the typically nonlinear adsorption of the components, but also dispersive effects due to mass transfer resistances, axial dispersion, etc. Unfortunately, under typical practical conditions their model equations have to be solved numerically. This makes them less useful when aiming at general insight into process behavior, performing basic process design or developing new concepts.

Equilibrium theory provides a more fundamental approach for the analysis and basic design of chromatographic processes. This powerful framework is equally applicable to conventional fixed-bed processes, countercurrent schemes as well as reactive chromatography. It is based on the strong simplifying assumptions of locally established thermodynamic equilibrium and negligible dispersive effects. These lead to simpler formulations of the governing mass balances for which ana-

lytical solutions can be derived.

The theory has been developed within more than 60 years. Wilson [101] realized in 1940 the existence of self-sharpening fronts in chromatograms, Weiss [102] noted the dispersive waves. DeVault [103] explained the shock physically and described the effects of competition and displacement considering convex upward and downward isotherms. Glückauf [104–106] solved the ideal model for sigmoidal and, importantly, for competitive Langmuir isotherms. The mathematical treatment was pushed forward by the concepts of weak solutions proposed by Lax [107] and that of coherence by Helfferich [108]. The theory arrived at a rather mature state with the comprehensive works by Helfferich [109] and Rhee and Amundson [110]. A more detailed historical overview is given in [111].

A summary of the mathematical fundamentals is found in the books by Rhee, Aris, and Amundson [84, 112]. Less mathematically oriented readers interested in constructing chromatograms might prefer the well-known book by Guiochon *et al.* [1]. Of particular relevance for this work are also the design methods for SMB processes developed by Mazzotti *et al.* [113–117] and the extension to reactive chromatography published by Kienle *et al.* [85, 86].

Below the main principles of equilibrium theory are summarized as far as they are required to understand the analysis and design methods for the different processes discussed in later chapters.

## Single Column Chromatography

Under the assumption of established thermodynamic equilibrium and neglecting any dispersive effects, the mass balance equations for a single chromatographic column as in Fig. 2.1 can be written as

$$\frac{\partial c_i}{\partial t} + \frac{1 - \varepsilon}{\varepsilon} \frac{\partial q_i}{\partial t} + u \frac{\partial c_i}{\partial x} = 0, \quad i = (1, N). \quad (2.1)$$

Equations (2.1) constitute the ideal or equilibrium model of chromatography. The independent time and space variables are  $t$  and  $x$ , while the dependent variables  $c_i$  and  $q_i$  are the fluid phase concentrations of component  $i = 1 \dots N$ , and the corresponding solid phase loadings, respectively.  $u = Q/(\varepsilon A)$  is the interstitial fluid velocity with  $\varepsilon$  as the bed porosity<sup>1</sup>

<sup>1</sup>For the sake of simplicity, this derivation assumes a non-porous stationary phase. Equations (2.1) hold for porous particles when replacing  $\varepsilon$  with the total porosity  $\varepsilon_t = \varepsilon_b + (1 - \varepsilon_b)\varepsilon_p$ , where  $\varepsilon_b$  and  $\varepsilon_p$  are the bed and the intra-particle porosity, respectively, and by setting  $u = Q/(\varepsilon_t A)$ .

In many cases it is useful to re-formulate the model using the dimensionless time and space variables  $\tau = tu/L$  and  $z = x/L$ , where  $L$  is the column length. With the phase ratio  $F = (1 - \varepsilon)/\varepsilon$ , one obtains

$$\frac{\partial}{\partial \tau} (c_i + Fq_i) + \frac{\partial c_i}{\partial z} = 0, \quad i = (1, N). \quad (2.2)$$

The loadings  $q_i$  in Eq. (2.2) are related to the fluid phase concentrations by a thermodynamic equilibrium expression. For isothermal adsorption-based processes, this is called adsorption isotherm (for the sake of brevity here usually denoted as “isotherm”),

$$q_i = q_i(c_1, c_2, \dots, c_N), \quad i = (1, N). \quad (2.3)$$

In general adsorption isotherms have to be determined experimentally. A number of specialized techniques exists for this task reviewed recently by Seidel-Morgenstern [118]. An accurate measurement – in particular of competitive equilibria – can be tedious, but the examples and methods to be discussed in this work will underline that significant efforts are justified for this.

Two main types of nonlinear and competitive isotherms will be considered below. The first is the famous model by Langmuir [119] which describes interactions with homogeneous surfaces. For competitive multi-component systems it is written as

$$q_i = q_{S,i} \frac{b_i c_i}{1 + \sum_j b_j c_j}, \quad i, j = (1, N), \quad (2.4)$$

with  $q_{S,i}$  as the saturation capacities of the components and  $b_i$  as interaction parameters. Equations (2.4) constitute the equilibrium function most frequently applied in preparative chromatography.

The second isotherm to be used is the bi-Langmuir model [120]. This accounts for adsorption onto heterogeneous surfaces by assuming two different types *I* and *II* of Langmuir adsorption sites. It is particularly suitable for enantiomeric systems, since it allows describing separately a selective chiral and a non-selective achiral interaction [121]. In competitive multi-component form it is given by

$$q_i = q_{S,i}^I \frac{b_i^I c_i}{1 + \sum_j b_j^I c_j} + q_{S,i}^{II} \frac{b_i^{II} c_i}{1 + \sum_j b_j^{II} c_j}, \quad i, j, k = (1, N). \quad (2.5)$$

Note that thermodynamic consistency of Eqs. (2.4) and (2.5) is guaranteed only if the saturation capacities  $q_S$  are equal for all components. However, meeting this criterion is not required for the binary separations considered in this work.

Equations (2.2) form a reducible set of homogeneous quasilinear partial differential equations (PDEs) of first order. The equations are nonlinearly coupled if

Eqs. (2.3) are competitive equilibria. It is important to realize that the type of the PDE system and the nature of the solutions depend on this equilibrium function. The PDE system (2.2) is called *strictly hyperbolic*, if the Jacobian matrix  $J$ , that consists of the partial derivatives of the equilibrium function, has  $N$  real and distinct eigenvalues and  $N$  linearly independent eigenvectors. It is denoted just as *hyperbolic* or *weakly hyperbolic* if  $J$  has multiple real eigenvalues, as *parabolic degenerate* for multiple real eigenvalues and less than  $N$  independent eigenvectors and, finally, as *elliptic* for complex eigenvalues Equations (2.2) [122].

The theory applied here is most developed for strictly hyperbolic systems. It can be shown that strict hyperbolicity is always guaranteed for the Langmuir model in Eq. (2.4) [123]. This holds also under thermodynamically inconsistent conditions with different saturation capacities. Exceptions exist only in so-called watershed points located on the boundary of the concentration space. More recently in [124] strict hyperbolicity was also proven for the modified Langmuir model, which extends Eq. (2.4) by linear terms. For bi-Langmuir isotherms, Eq. (2.5), it was found in [124] that generally hyperbolicity depends on both, isotherm parameters *and* concentrations, and may fail. However, systems with  $N$  components are hyperbolic if the saturation capacities on each adsorption site  $j = (I, II)$  are equal and positive. Moreover, for two-component systems,  $N = 2$ , strict hyperbolicity is given for positive  $q_{S,i}^j$  and  $b_i^j$ . Like for Langmuir isotherms, multiple eigenvalues can occur only on the concentration axes. The binary separation problems with bi-Langmuir isotherms discussed in this work fall into this category.

A particular property of the model Eqs. (2.2) is that they describe wave phenomena. If the equilibrium Eq. (2.3) for a single solute is a nonlinear function  $q = q(c)$ , the migration velocity of each concentration value depends on the concentration itself. Moreover, if the equilibria in a multi-component system are competitive,  $q_i = q_i(c_1, c_2, \dots)$ , as is the case in Eqs. (2.4) and (2.5), the migration velocities of all concentrations depend on the concentrations of all present adsorbing species. This gives rise to the emergence of the peculiar phenomena like dispersed waves and shock fronts that are characteristic for nonlinear chromatography.

In order to simulate a chromatographic process, the model equations have to be solved for a correspondingly defined initial value problem or a succession thereof. For example, a typical elution process in batch chromatography can be defined as two consecutive problems with constant initial conditions and a step-change in the boundary conditions. The first of these so-called Riemann problems corresponds to a step of the inlet concentrations from the pure eluent to the feed while the column is completely regenerated. The second problem is the regeneration of the now pre-loaded column by feeding again pure eluent. More complex scenarios can also be studied.

The solution of Riemann problems for such systems can be accomplished by the method of characteristics. For details the reader is referred to, for example, [84, 112]. To understand the procedures applied in this work it is sufficient to know that any discontinuity in the boundary or initial conditions will be resolved in at most  $N$  (as the number of components) simple waves, shocks, or contact discontinuities. For the isotherm models considered below, their propagation velocities, and thus the complete solution, can be calculated from the eigenvalues and eigenvectors of the Jacobian matrix  $J$ .

Let us consider a two-component system described by the Langmuir model (2.4) to elucidate the solution procedure. In this case the Jacobian  $J$  is given by

$$J = \begin{bmatrix} q_{11} & q_{12} \\ q_{21} & q_{22} \end{bmatrix} = \begin{bmatrix} \frac{a_1(1+b_2c_2)}{N^2} & -\frac{a_1b_2c_1}{N^2} \\ -\frac{a_2b_1c_2}{N^2} & \frac{a_2(1+b_1c_1)}{N^2} \end{bmatrix}, \quad (i = 1, 2) \quad (2.6)$$

with  $q_{ij} = \frac{\partial q_i}{\partial c_j}$ ,  $N = 1 + b_1c_1 + b_2c_2$ ,  $a_i = q_{S,i}b_i$ .

In the following  $i = 1$  and  $i = 2$  will denote the weaker and the stronger adsorbing component, respectively.

The eigenvalues  $\lambda$  of  $J$  are calculated from the following equation,

$$\lambda^2 - (q_{11} + q_{22})\lambda + q_{11}q_{22} - q_{12}q_{21} = 0, \quad (2.7)$$

where the two solutions are ordered as  $\lambda_1 < \lambda_2$ . These eigenvalues define the slopes of characteristics  $C$  in the physical plane  $(z, \tau)$ , and are inversely proportional to the characteristic propagation velocity  $v_c$  of a given composition in a *simple wave*,

$$v_{c_j} = \frac{1}{1 + F\lambda_j}, \quad (j = 1, 2). \quad (2.8)$$

Note that the propagation velocities in the dimensionful  $(t, x)$  plane are obtained by multiplying  $v_{c_j}$  with the interstitial velocity  $u = Q/(\epsilon A)$ .

Which of the two velocities  $v_{c_1}$  and  $v_{c_2}$  in Eq. (2.8) actually represents the valid solution depends on the initial and boundary conditions. In this context the eigenvectors of the matrix  $M = I + FJ$ , where  $I$  is the identity matrix, provide a useful tool. The eigenvectors define characteristics  $\Gamma$  in the concentration space. For the binary system considered here they can be calculated from the eigenvalues of  $J$  as

$$\Gamma_{\pm} : \frac{dc_1}{dc_2} = \frac{\lambda_{1/2} - q_{22}}{q_{21}} = \xi_{\pm}. \quad (2.9)$$

From Eq. (2.7) one finds

$$\xi_{\pm} = \frac{q_{11} - q_{22}}{2q_{21}} \pm \sqrt{\left(\frac{q_{11} - q_{22}}{2q_{21}}\right)^2 + \frac{q_{12}}{q_{21}}}.$$

The characteristics span a network in the concentration domain, the so-called hodograph space. They pre-define the paths that can be taken by simple wave solutions. It is worth emphasizing that the path grid itself depends on the isotherm parameters only and is, thus, independent of the process conditions. The latter, represented by the initial and boundary conditions, determine *which* of the two paths that exist in each composition  $(c_1, c_2)$  is taken by the solution (see below).

The expressions above hold *for simple waves only*. It is well known that for hyperbolic systems as given here by using the Langmuir isotherm also *shocks* can develop. These represent discontinuous, so-called weak solutions of the PDE system. Their velocity is found by replacing the eigenvalue in Eq. (2.8) by the finite differences

$$\tilde{\lambda} = \frac{[q_1]}{[c_1]} = \frac{[q_2]}{[c_2]}, \quad (2.10)$$

where the brackets  $[\cdot]$  denote the differences of concentration and loadings left and right of the shock. This equation is known as jump or Rankine-Hugoniot condition from fluid mechanics [125].

The consequence of this is that in a given composition  $P$  there exist two shock paths, denoted here as  $\Sigma_+$  or  $\Sigma_-$ , that connect  $P$  to two loci to be determined from Eq. (2.10). The two shock paths are tangent to the  $\Gamma$  characteristics in  $P$ . Note that the  $\Sigma$  are generally different from the  $\Gamma$  characteristics. In the case of Langmuir isotherms, however, both the  $\Sigma$  and  $\Gamma$  are straight lines and, thus, fall together.

From Eq. (2.10) follows for the velocities of the shocks,

$$v_{s_j} = \frac{1}{1 + F \frac{[q_j]}{[c_j]}}, \quad (j = 1, 2). \quad (2.11)$$

Again, dimensionful velocities are obtained by multiplying  $v_{s_j}$  with the interstitial velocity  $u$ .

An illustration of the solution procedure for a full chromatographic cycle is given in Fig. 2.3. First the feed mixture ( $F$ ) is injected into the initially empty column (state  $I$ ). Later the column is regenerated by interchanging  $F$  and  $I$ .

The solution is now found by taking from the initial condition  $I$  first the “fast path” (corresponding to the smaller eigenvalue  $\lambda_1$  and thus to the higher velocity) until the slower path ( $\lambda_2$ , lower velocity) is reached in  $P_1$  that gives a connection

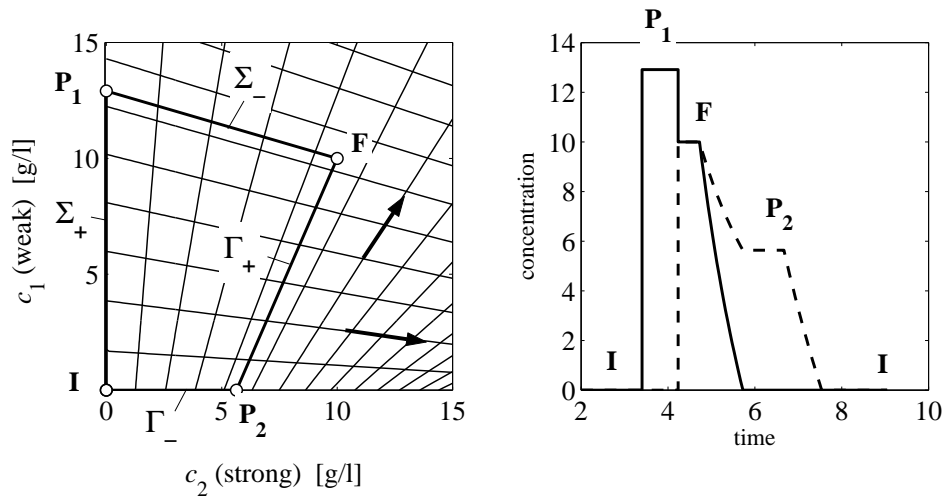


**Figure 2.3** – Example for a complete chromatographic cycle for a large injection of a mixture ( $F$ ) onto an empty column ( $I$ ) for Langmuir isotherms. Left – hodograph plane. The  $\Gamma_+$  (“fast paths”) are the characteristics progressing towards the upper right, the  $\Gamma_-$  (“slow paths”) towards the lower right of the diagram, respectively. The arrows mark the directions along the characteristics in which the eigenvalues  $\lambda_j$  decrease. Right – corresponding chromatogram.

Parameters:  $a_1 = 2.0$ ,  $a_2 = 3.0$ ,  $b_1 = b_2 = 0.02 \text{ L/g}$ ,  $c_{F,i} = 10 \text{ g/L}$ ,  $c_{I,i} = 0$ .

to the boundary condition  $F$ . If along a path the eigenvalue decreases (i.e., in the direction of the arrows in the figure), the velocity increases and the corresponding transition is a shock. This is the case here for both paths during the loading, which are correspondingly a  $\Sigma_+$  and a  $\Sigma_-$ .

In the elution step from  $F$  to  $I$ , the initial conditions are now given by  $F$ . Since first the fast path has to be followed, one has to move from  $F$  downwards along this to find a connection to  $I$ . Along the route,  $\lambda_2$  increases (the velocity decreases), which corresponds to having a simple wave on a  $\Gamma_+$ . The same holds along the slow  $\Gamma_-$  from  $P_2$  to the state  $I$ .

At the intersections of the characteristics the plateaus  $P_1$  and  $P_2$  develop provided the injection is sufficiently large. The corresponding chromatogram in the right of the figure follows now from the expressions for the velocities of the simple waves and shocks above, with the concentration values now known from the hodograph plot. It should be noted that for smaller injections the waves will interact with each other, causing an erosion of these plateaus. The solution is still possible (see e.g. [PII-2]) but is somewhat more involved.

Before considering also countercurrent chromatography, an alternative approach should be mentioned. The  $\omega$ -transform [84] orthogonalizes the characteristics in the hodograph plane. This is particularly interesting when analyzing systems with

a larger number of components, because the construction rules for the solutions can be conveniently implemented in the orthogonalized variables.

The following definition creates for Langmuir isotherms a one-to-one mapping between the concentrations in the hodograph plane and the  $\omega$ -values in the corresponding domain,

$$\sum_{i=1}^N \frac{q_i b_i}{a_i - \omega} = 1, \quad (i = 1 \dots N) \quad (2.12)$$

The solution can be fully constructed in the  $\omega$ -space since also the velocities can be expressed in terms of the  $\omega_j$  values. The latter are related to the eigenvalues  $\lambda_j$  by

$$\omega_j = \lambda_j \left( 1 + \sum_j b_j c_j \right), \quad (j = 1 \dots N). \quad (2.13)$$

An example for the application of the  $\omega$ -transform is given in Section 3.1.

## Simulated Moving Bed Chromatography

Applying equilibrium theory to SMB chromatography facilitated the development of the “triangle theory” as the most important tool for the basic design such this process for various types of adsorption equilibria and operating concepts, see *e.g.* [113–117, 126, 127]. It is particularly popular for the relevant case of Langmuir isotherms, since there it yields simple explicit equations for the optimal operating conditions [128]. Furthermore, the determined separation regions allow for a generic view on the operating regime.

To allow for an easier understanding of the methods derived later, below a brief outline is given on the underlying principles of applying equilibrium theory to this type of problem.

In the context of equilibrium theory, it is common to consider the fully continuous true moving bed (TMB) concept illustrated in Fig. 2.4 as an approximation of the more complex periodically operated SMB process. The mass balances for a TMB process read, written in the direction of the fluid phase flow,

$$\frac{\partial}{\partial \tau} (c_i + F q_i) + \frac{\partial}{\partial z} (m^j c_i - q_i) = 0 \quad (2.14)$$

with  $(i = 1, 2), (j = I \dots IV),$

with  $\tau = t F u_S / L$  and  $z = x / L$  as dimensionless time and space variables,  $u_S$  the interstitial solid phase velocity<sup>2</sup>, and  $L$  as the section length. The  $m^j$ -values in

<sup>2</sup>Note that  $u_S$  is defined as  $u_S = Q_S / [(1 - \varepsilon) A]$ .

Eq. (2.14) represent the most important design parameters in countercurrent chromatography. They are defined as the dimensionless ratio of the liquid flow rate  $Q^j$  and the solid flow rate  $Q_S$  in the  $j$ th section of a TMB process and relate to the flow rates in the corresponding SMB process by, see *e.g.* [128],

$$m^j = \frac{Q^j}{Q_S} = \frac{u^j}{F u_S} = \frac{Q^{j, \text{SMB}} t_S - \varepsilon V}{V(1 - \varepsilon)}, \quad j = (I \dots IV) \quad (2.15)$$

where  $t_S$  is the switching time of the SMB unit and  $V$  the column volume.

Equations (2.14) are largely analogous to those for the batch column in Eqs. (2.2). In fact the single column is a special case of the TMB concept with a solid flow rate of zero. Therefore, many of the solution principles for single columns can be applied directly to TMB processes.

In analogy to the single column where the velocities for simple waves and shocks are given by Eqs. (2.8) and (2.11), holds for the characteristic velocity in a TMB section in case of a *simple wave*,

$$v_{c,j} = \frac{1 - \frac{1}{m} \lambda_j}{1 + F \lambda_j}, \quad (j = 1, 2), \quad (2.16)$$

and for a *shock*,

$$v_{s,j} = \frac{1 - \frac{1}{m} \frac{[q_j]}{[c_j]}}{1 + F \frac{[q_j]}{[c_j]}}, \quad (j = 1, 2). \quad (2.17)$$

Physical migration velocities are again obtained by multiplying the  $v$  with  $u$ . Note that, when introducing  $m = u/(F u_S)$  into Eqs. (2.16) and (2.17), it immediately becomes apparent that the velocities for batch chromatography given in Eqs. (2.8)

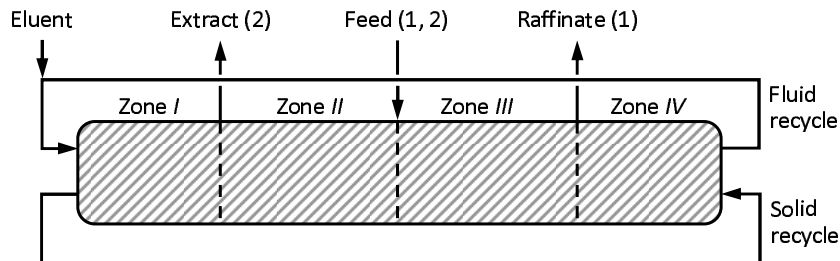


**Figure 2.4** – Schematic representation of a true moving bed (TMB) process. The continuous concept is a simplified approximation of the periodically operated SMB process in Fig. 2.2.

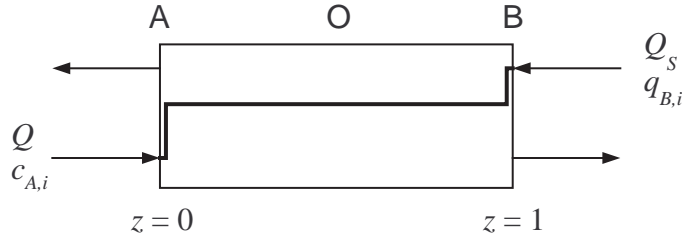


**Figure 2.5** – Riemann problem for a single TMB section. The incoming streams and their compositions – the state  $A$  of the liquid phase entering from the left and the state  $B$  of the solid phase from the right – determine the values of the internal state  $O$  and at the outlets. The illustrated profile corresponds to a simple wave in steady state with two boundary discontinuities.

and (2.11) represent special cases where  $u_S = 0$ .

Also in the TMB process the simple waves map onto the  $\Gamma$  characteristics and the shocks onto the  $\Sigma$  paths, respectively. It is important to realize that the pathgrid spanned by the  $\Gamma$  characteristics in the hodograph plane is the same for TMB and batch processes, since it depends on the isotherm parameters only.

The actual course of the solution is found again by considering a Riemann problem, now for a single section as illustrated in Fig. 2.5. The incoming streams  $c_{A,i}$  and  $q_{B,i}$  are the boundary conditions that have to be connected by two characteristics or shocks, respectively, in the hodograph plane. The correct “pair” is found by comparing the eigenvalues or, alternatively, the  $\omega$ -values for the boundary conditions, see [84].

In steady state only the state  $O$  can prevail in the interior of the section for which the velocity is zero. The position of  $O$  along the admissible path is determined by the  $m$ -value. Setting  $v_{c,j} = 0$ , one immediately finds from Eq. (2.16) for  $O$  on a  $\Gamma_+$  characteristic,

$$m = \lambda_1, \quad (2.18)$$

and for  $O$  on a  $\Gamma_-$  characteristic,

$$m = \lambda_2. \quad (2.19)$$

For the shocks one obtains from Eq. (2.17),

$$m = \frac{[q_j]}{[c_j]}. \quad (2.20)$$

Different ranges hold for the  $m$ -value in which  $O$  lies either on the  $\Gamma_+$  ( $\Sigma_+$ ),  $\Gamma_-$  ( $\Sigma_-$ ), at their intersection, or in either one of the boundary conditions, respectively.

The states leaving the zone do not have to be in equilibrium with the incoming streams (“boundary discontinuities”). They are obtained from balances around the top or bottom of the zone.

Detailed rules for constructing the complete solutions for transient and steady-state problems are given in [84]. To design the process in Fig. 2.4 the steady-state solutions for the four zones are combined with the material balances between and at the boundaries of the zones. However, additional assumptions are required to solve the equations. For the example of the complete separation of two components with Langmuir isotherms, the linear characteristics in conjunction with requiring complete regeneration in zones *I* and *IV* facilitated deriving the well-known explicit separation region in the  $m^{II}$ - $m^{III}$  domain, see *e.g.* [128]. More recently explicit separation regions were also obtained for the concept of generalized Langmuir isotherms [126, 127].

## Reactive Chromatography

For reactive chromatographic processes the mass balances are sets of heterogeneous partial differential equations, which complicates the situation significantly. However, by simplifying assumptions it is possible to transform the heterogeneous PDE system into a homogeneous one. Based on this the theoretical treatment above was extended to some special cases in [84].

A useful method evolves if the limiting case of simultaneously established adsorption and reaction equilibrium can be assumed. By introducing transformed variables based on the stoichiometry, as suggested by Doherty *et al.* for reactive distillation [129], various scenarios can be studied also in chromatographic reactors [85, 86]. Suitably defined variables eliminate the unknown reaction rates from the balance equations and thereby render the PDE system homogeneous, whereby the dimension of the problem reduces by the number of reactions [85]. The same solution procedures as in the non-reactive cases are applicable.

This approach is pursued in Chapter 5 for an isomerization reaction performed in an integrated SMB process.

Another aspect are heat effects that arise when in adiabatic operation of chromatographic columns. Heat effects have been studied exhaustively for non-reactive systems by Rhee *et al.* [84, 130], who introduced energy contents as transformed variables that render the system analogous to one with an additional species. The application of similar variables to reactive systems is discussed in Chapter 5.



# Chapter 3

## Advanced Operating Modes

### 3.1 Batch Chromatography with Adsorbing Additives

Additives or modifiers are frequently applied in preparative chromatography, for example, to improve the separability of the compounds or to stabilize the pH value. If such additive is *adsorbing competitively*, the presence of this additional component can give rise to significant nonlinear effects. Depending on its adsorptivity, resulting peak shapes can be difficult to interpret. Examples are peaks that imply a change from Langmuirian to anti-Langmuirian adsorption behavior although all compounds have Langmuir isotherms [131–133], or peak splitting caused by a modifier [134, 135]

In the enclosed manuscript [PII-4] three enantiomeric systems are investigated in detail wherein the additive (a buffer compound) has either weakest, intermediate or strongest adsorptivity in a set of competitive bi-Langmuir isotherms. The paper aims in particular at identifying possible benefits of adsorbing additives in batch chromatography, and gives suggestions regarding the optimal operation. A particular finding is that it is mandatory to take into account carefully the elution profile of the additive – which is often not visible in detector signals – when designing repetitive process cycles.

Apart from the results of this study it is useful to elucidate such situation in the frame of equilibrium theory. As an introductory example, let us consider the hodograph for a binary system with Langmuir isotherms in Fig. 2.3. It is clear that saturating an initially empty column with a binary mixture will cause two shock transitions. However, when injecting  $F: (c_{F,1} = 10, c_{F,2} = 0)$ g/L onto a column initially saturated with  $I: (10, 10)$ g/L, the solution will first follow the  $\Gamma_+$  characteristic from  $I$  in the direction of decreasing velocity (*i.e.* downwards), before it

**Table 3.1** – List of transitions in the  $\omega$  space for the complete chromatographic cycle of a ternary separation. Transitions (arrows) from states (1) through (4) correspond to loading the feed  $F$  onto the column with initial conditions  $I$ . Transitions (4) through (7) mark the elution back to state  $I$ .

I = (1)	(2)	(3)	(4) = F	(5)	(6)	(7) = I
$\omega_{I,1}$	$\rightarrow \omega_{F,1}$	$\omega_{F,1}$	$\omega_{F,1}$	$\rightarrow \omega_{I,1}$	$\omega_{I,1}$	$\omega_{I,1}$
$\omega_{I,2}$	$\omega_{I,2}$	$\rightarrow \omega_{F,2}$	$\omega_{F,2}$	$\omega_{F,2}$	$\rightarrow \omega_{I,2}$	$\omega_{I,2}$
$\omega_{I,3}$	$\omega_{I,3}$	$\omega_{I,3}$	$\rightarrow \omega_{F,3}$	$\omega_{F,3}$	$\omega_{F,3}$	$\rightarrow \omega_{I,3}$

moves along a  $\Gamma_-$  into  $F$ . The resulting transitions are both simple waves, creating a “scent” of anti-Langmuirian behavior. This underlines that the solution depends not only on the adsorption isotherms, but just as well on the initial and boundary conditions. Along similar arguments also various other “bizarre” situations can be fully explained.

It should be clear from the simple binary example above that an interesting elution behavior is to be expected for ternary systems in which one component, the additive, is present in the initial conditions of the column. For the sake of simplicity the following example will rely on Langmuir isotherms, Eq. (2.4), which were fitted to the bi-Langmuir isotherms, Eq. (2.5), reported in [133]. It was found useful to determine the solution paths for this ternary problem using the  $\omega$  transform. As explained in Section 2.3 this orthogonalizes the composition paths of the chromatographic cycle.

The  $\omega$  transform results in simple construction rules for chromatograms that can be summarized in four steps: *i*) *Transformation* of initial and boundary conditions  $I$  and  $F$  into their  $\omega$  coordinates by determining the  $N = 3$  roots of Eq. (2.12) and sorting the elements of  $\omega_I$  and  $\omega_F$  in increasing order. *ii*) The *order of transitions* corresponds to the order of the elements of the  $\omega$  values, as is illustrated in Table 3.1. *iii*) The *type of transition* is found by comparing the corresponding  $\omega$  values. For example, if for the step from (1) to (2) in Table 3.1  $\omega_{I,1} < \omega_{F,1}$  this corresponds to a simple wave, while for  $\omega_{I,1} > \omega_{F,1}$  a shock occurs. *iv*) The velocities are calculated from Eqs. (2.8) through (2.12) and the chromatogram is constructed. Note that for this illustrative example the case of wave interactions not considered.

The example shown in Fig. 3.1 corresponds to a large injection of the enantiomers of Alprenolol onto an analytical Chirobiotic T column [133]. The column is initially equilibrated with the eluent wherein the strongest adsorbing additive triethyl ammonium acetate is present as the only adsorbing component. The elution profiles calculated by the method above match closely those obtained numerically from an equilibrium-dispersive model for the Langmuir isotherms. For comparison the

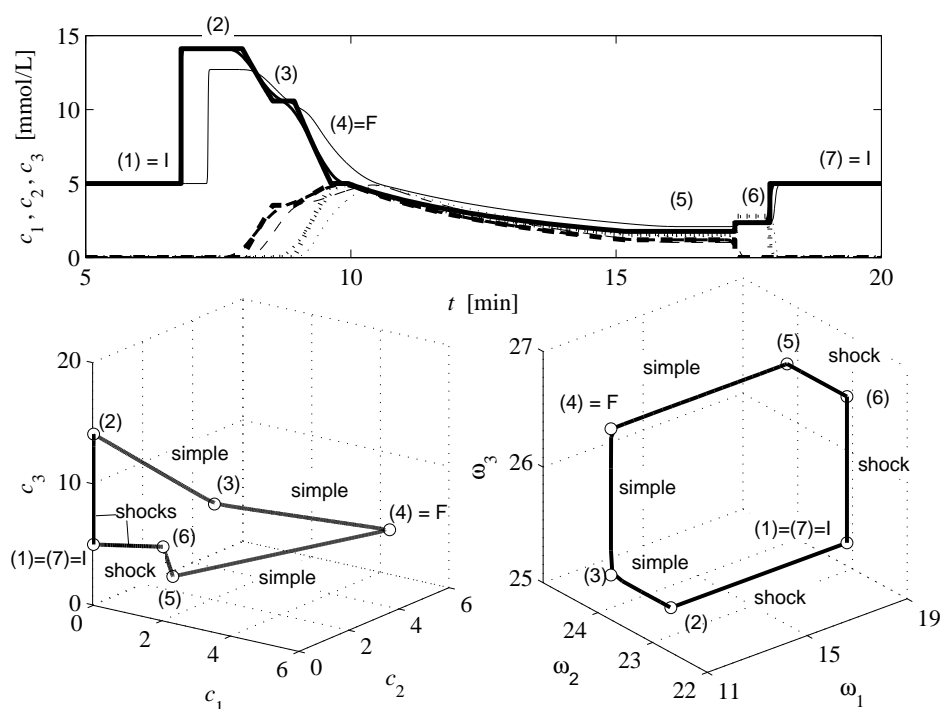


**Figure 3.1** – Separation of two enantiomers by batch chromatography in the presence of an adsorbing additive. Chromatograms at the column outlet (top), in the hodograph plot and in the  $\omega$  domain (bottom). The additive (solid lines) adsorbs strongest, the enantiomers intermediately (dotted) and weakest (dashed), respectively. Thick lines – solution by equilibrium theory, re-fitted Langmuir isotherms; medium – equilibrium-dispersive model corresponding to 11000 stages, Langmuir; thin – same model, bi-Langmuir.

Parameters:  $V_F = 7$  mL,  $c_F = (5, 5, 5)$  mmol/L,  $c_I = (0, 0, 5)$  mmol/L. Re-fitted Langmuir isotherms:  $a_i = (22.75, 25.35, 27.86)$ ,  $b_i = (0.07335, 0.07367, 0.1055)$ . bi-Langmuir isotherms from [133]; for other parameters see [PII-4].

figure shows also the profiles for the original bi-Langmuir parameters given in [133]. The results closely reflect the numerical and experimental results reported for this system in Fig. 5a [133] and Fig. 3a [PII-4].

The transitions for the complete cycle in this “strongly distorted” chromatogram are: shock – simple wave – simple wave for loading, and simple wave – shock – shock for regeneration, respectively. This is accompanied by a pronounced tag-along in the simple wave from state (4) to (5). Another interesting aspect is that the chromatogram starts with a pronounced pure component “ghost peak” of the *strongest* adsorbing additive. This can be explained by the fact that the initial concentration  $c_{I,3}$  lies above the two watershed points on this axis at  $(0, 0, 0.939)$  and  $(0, 0, 2.129)$  mmol/L. This part of the  $c_3$  axis is a  $\Gamma_+$  (or  $\Sigma_+$  path) characteristic which is taken first in direction of increasing  $c_3$  into point (2), before a  $\Gamma_-$  is taken

from (2) into (3).

The lower part of Fig. 3.1 reveals the usefulness of the  $\omega$  transform for ternary systems. While it is difficult to interpret the hodograph representation (bottom, left), the paths in the  $\omega$  plane (bottom, right) are easy to evaluate.

For more general design purposes a formulation appears desirable that accounts also for wave interaction. On the other hand, it might be of limited use due to the fact that most of the observed shocks are not very pronounced. Very high stage numbers are required to take advantage of, for example, the two separate final shocks between states (5) and (7) in Fig. 3.1. It is questionable if a column with such high efficiency will exhibit a pressure drop suitable for an industrial application.

As for the bi-Langmuir isotherms originally underlying the parameters used here, the  $\omega$  transform is not applicable. In such case the solution procedures described in Section 2.3 have to be applied. Furthermore, it should be verified that the system is strictly hyperbolic in the concentration domain of interest, which is not always the case for ternary bi-Langmuir systems [124].

## 3.2 Steady-State Recycling Chromatography

When performing difficult chromatographic separations of valuable components it is a serious challenge to maximize the recovery yield. One of the options for this is closed-loop recycling (CLR) [9–11] where a partially separated elution profile is recycled over the column several times until sufficient separation is achieved. This can be accelerated to a certain extent by “peak shaving” [10] and “alternate pumping” [136]. Yet, CLR processes achieve only low productivities.

A more promising approach, in particular for binary separations, is steady-state recycling (SSR) chromatography [12]. In SSR processes a certain amount of fresh feed is added to each recycle fraction after collecting the purified leading and trailing edges of the elution profile (peak shaving). The process is operated such that it attains a periodic steady state after a number of cycles.

The main challenge in SSR chromatography is to design the process. There are two major process concepts. The closed-loop mode (CL-SSR) [13] attempts to preserve the partially separated elution profile. This is difficult to design because of the resulting dynamic injection profile. Here the classical mixed-recycle mode (MR-SSR) [12] is studied. In MR-SSR the recycle fraction is *mixed* with the fresh feed before the injection, which simplifies the design.

In the two enclosed manuscripts [PII-2] and [PII-3] new shortcut methods are proposed that allow for a rapid design and evaluation of MR-SSR processes for arbitrary purity requirements.

### 3.2.1 Design and Performance Under Ideal Conditions

The design task addressed here is to predict *a priori* the four cut times that lead to two product fractions that fulfill the purity requirements in steady state. This situation is illustrated in Fig. 1 [PII-2].

The operation principle of MR-SSR as shown in the figure corresponds to a scenario with piecewise constant initial and boundary conditions, for which equilibrium theory provides a powerful methodology. In the case of Langmuir adsorption isotherms a complete chromatogram can be constructed rather easily for a given column setup if the required operating parameters – flow rate, injection volume, and injection composition – are known, see Section 2.3. The disturbing aspect here is that the chromatogram at steady state is of interest, for which the injection composition is not known.

This problem can be solved without performing dynamic simulation. In [PII-2] a method is proposed that predicts directly the steady state and the relevant cut times for arbitrary purity requirements for the case of Langmuir isotherms.

An analysis based on equilibrium theory revealed that the composition of the recycle always remains on the  $\Gamma_+$  characteristic through the fresh feed, see Fig. 2 [PII-2], and that the amounts in the second product fraction are invariant from cycle to cycle. Furthermore, in a binary separation without waste fractions specifying the two purity requirements unambiguously fixes the relative mass fluxes in the two outlets relative to the feed amounts [137]. Combining these information with the “construction rules” of equilibrium theory yields largely explicit equations for the four cut times and the composition of the injection at steady state.

The approach makes analysing the performance of MR-SSR straightforward, because the injection volume remains as the only free operating parameter. In this context it was proven that under equilibrium conditions, *i.e.* negligible dispersion, MR-SSR guarantees a lower solvent consumption and higher product concentrations, but not the productivity of batch chromatography. These results are shown graphically in Fig. 4 [PII-2]. It will be demonstrated later that under dispersive conditions even the productivity of MR-SSR can exceed considerably that of a batch system.

Finally, an interesting aspect is that the knowledge of the injection composition at steady state permits eliminating the startup period of the process. This is done

by simply performing the very first injection(s) with a prepared mixture of that composition.

### 3.2.2 Design and Performance Under Nonideal Conditions

Under industrial conditions the assumptions made in the previous section will usually not hold any more. Dispersion can be significant and adsorption isotherms do not necessarily follow the Langmuir model. Solutions from equilibrium theory are useful here for basic design. The detailed design of recycling processes requires more efforts and is typically accomplished on the basis of the more detailed dynamic models described in Section 2.2 [10, 11, 138–141]. It should be realized that the cyclic and accumulative nature of SSR processes requires laborious experimental determination of very accurate model parameters.

Against this background an extension of the shortcut design method above to non-ideal systems was proposed in [PII-3]. The method exploits the fact that for favourable isotherms the rear part of an overloaded chromatogram is largely independent of the injection volume. This holds even in the presence of strong dispersive effects, provided the isotherms are sufficiently nonlinear.

This common practical observation is exploited in [PII-3] insofar as that the numerical integration along the  $\Gamma_+$  characteristic in the equilibrium design method above is replaced by simply integrating the rear part of a chromatogram. The result is a shortcut design method for MR-SSR chromatography under dispersive conditions that is not restricted to Langmuir isotherms, but applies to systems with favourable isotherms in general. The method holds again for arbitrary purity requirements and requires as input only a single experimental or simulated chromatogram. Isotherm parameters have not to be measured, and a dynamic simulation is not necessarily required.

The approach was validated for the separation of two cycloketones on a polymeric stationary phase. This system exhibits strongly nonlinear bi-Langmuir isotherms and a low column efficiency with 30 theoretical stages only.

A parametric study using a transport-dispersive model demonstrated that the calculated cut times are very close to the required values. The purity of the second fraction is always met with high accuracy, and only minor refinements of the cut times suffice to correct purity deviations of the first fraction, see Tab. 1 [PII-3].

These findings were supported in experimental investigations using the setup in Fig. 3.2. The purities in Tab. 3 [PII-3] are in all investigated scenarios close to the design specifications. It was also shown that the duration of the startup phase depends strongly on the desired product purity. High purity requirements, Fig. 5 [PII-3], cause a much longer startup phase than lower values, Fig. 6 [PII-3]. Although the

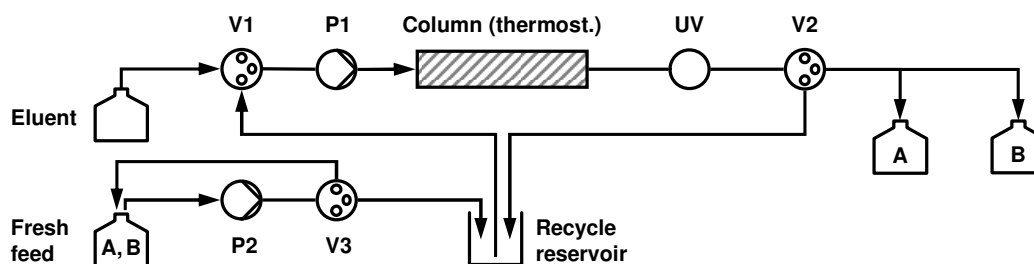


**Figure 3.2** – Experimental setup for MR-SSR chromatography. Valve  $V1$  controls injection and eluent flow,  $V2$  performs product collection and recycling,  $V3$  controls addition of fresh feed. The latter is pumped in a circle to eliminate possible failure of pump  $P2$  due to frequent activation. Simpler setups are possible and have been tested.

design method does not give information on the steady state injection composition, this can be determined experimentally and then again be used to eliminate the startup, as shown in Fig. 7 [PII-3].

The role of column efficiency for process performance was elucidated using the design method together with the model. The results in Fig. 8 [PII-3] demonstrate a superior performance of MR-SSR in comparison to batch chromatography.

The design method was also used successfully for designing a pharmaceutical enantioseparation, where one component exhibited a sigmoidal isotherm. The MR-SSR process was combined with a subsequent crystallization. The results are illustrated in Chapter 4.

## 3.3 Simulated Moving Bed Chromatography

### 3.3.1 Design for bi-Langmuir Isotherms

As already mentioned earlier, the separation of enantiomers has become a key application of SMB chromatography. An accurate modeling of the adsorption behavior of enantiomers frequently requires using the bi-Langmuir model, Eq. (2.5), since this allows a differentiation between chiral and non-chiral interactions of the solutes with the chiral stationary phase.

For the basic design of SMB processes for bi-Langmuir systems, a solution for the  $m^j$  values has been provided by Mazzotti and co-workers in the frame of the “triangle theory” [117]. In spite of the relevance of the application area, the application of this rigorous method is rarely reported in the literature. This might be attributed to the fact that some practitioners face difficulties in its implementation, since one of its steps requires a non-trivial numerical scheme (see below).

In [117] this was obviously anticipated and a simple explicit shortcut method was suggested. However, the accuracy of the latter appears rather limited. Below an alternative shortcut design method is proposed, which is also explicit but approximates the rigorous solution with higher accuracy.

For bi-Langmuir isotherms the design problem can be solved only numerically because here in principle the characteristics in the hodograph plane are curved. On the other hand, a strong curvature of the characteristics is hardly observed for most parameter sets of bi-Langmuir isotherms reported in the literature. The idea of the new shortcut method is, thus, to approximate a specific  $\Gamma_+$  characteristic by a straight line. This allows for a completely explicit solution. It is worth mentioning that the design method obtained such is *approximate* for bi-Langmuir, but *accurate* for Langmuir and modified Langmuir isotherms, respectively, where the characteristics are straight lines, *cf.* Fig. 2.3.

The shortcut approach follows, except for the simplification mentioned above, the rigorous solution in [117]. Below it will be summarized and illustrated. Figure 3.3 shows the solution in the hodograph plot (left) and the region of complete separation in the  $m^{II} - m^{III}$  plane (right) for the parameters reported in [117]. In [117] it was proven that for  $m^{III} = m_{\max}^{III}$ , which holds in the part *wr* of the boundary of the separation region, the states of the Riemann problem for zone *II*,  $D - M_2 - \beta$ , and those for zone *III*,  $D - M_3 - \gamma$ , intersect in point  $\beta = \gamma$ . Furthermore, the material balance around the feed *F* is a straight line  $\alpha - \beta - F$ . Since the characteristic are nonlinear curves, the states  $\beta$  and  $M_2$  have to be determined one from another through integration along the  $\Gamma_+$  that connects both states. Simultaneously a small system of nonlinear equations has to be solved that results from the separation conditions and the shock velocities in zone *III*.

It is readily observed in Fig. 3.3 (left) that for the considered parameters the  $\Gamma$  characteristics are indeed almost linear. Therefore, the  $\Gamma_+$  through the feed *F* basically coincides with the  $\Gamma_+$  that connects  $\beta$  and  $M_2$ . Since in  $M_2$  holds  $c_1 = 0$  [117], assuming that this  $\Gamma_+$  is a straight line gives for the approximated point  $M'_2$  in the hodograph plane

$$c_1^{M'_2} = 0, \quad (3.1a)$$

$$c_2^{M'_2} = c_2^F - \frac{c_1^F}{\xi_+^F}. \quad (3.1b)$$

where  $\xi_+^F$  is the local slope of the  $\Gamma_+$  in the feed point  $(c_1^F, c_2^F)$  according to Eq. (2.10). The partial derivatives  $q_{ij}$  in Eq. (2.10) can be calculated explicitly.

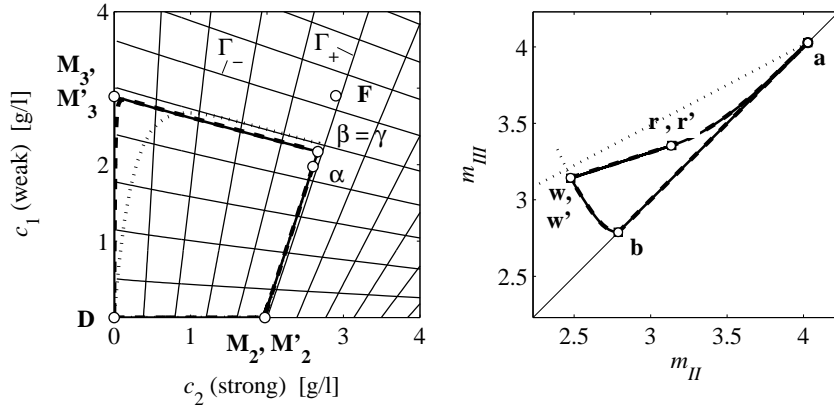


**Figure 3.3** – Application of rigorous and shortcut design methods to the bi-Langmuir isotherms used in [117]. Left – hodograph representation, right – region of complete separation in the  $m^{\text{II}}-m^{\text{III}}$  plane. Solid thick lines – rigorous solution [117], dotted – shortcut method in [117], dashed – proposed new shortcut method. Concentration profiles (left) obtained from a TMB model with 1000 stages/zone for the optimal operating point  $w$  predicted by each method.

Parameters:  $a_1^{\text{I}} = 2.688$ ,  $a_2^{\text{I}} = 3.728$ ,  $a_1^{\text{II}} = 0.1$ ,  $a_2^{\text{II}} = 0.3$ ,  $b_1^{\text{I}} = 0.0336\text{L/g}$ ,  $b_2^{\text{I}} = 0.0466\text{L/g}$ ,  $b_1^{\text{II}} = 1.0\text{L/g}$ ,  $b_2^{\text{II}} = 3.0\text{L/g}$ ,  $c_1^{\text{F}} = c_2^{\text{F}} = 2.9\text{g/L}$ ,  $m^{\text{I}} = 1.1$  ( $a_2^{\text{I}} + a_2^{\text{II}}$ ),  $m^{\text{IV}} = 0.01$ .

The Jacobian  $J$  for bi-Langmuir isotherms reads

$$J = \begin{bmatrix} q_{11} & q_{12} \\ q_{21} & q_{22} \end{bmatrix} = \begin{bmatrix} \frac{a_1^{\text{I}}}{N^{\text{I}}} + \frac{a_1^{\text{II}}}{N^{\text{II}}} - \frac{a_1^{\text{I}}b_1^{\text{I}}c_1}{N^{\text{I}2}} - \frac{a_1^{\text{II}}b_1^{\text{II}}c_1}{N^{\text{II}2}} & -\frac{a_1^{\text{I}}b_2^{\text{I}}c_1}{N^{\text{I}2}} - \frac{a_1^{\text{II}}b_2^{\text{II}}c_1}{N^{\text{II}2}} \\ -\frac{a_2^{\text{I}}b_1^{\text{I}}c_2}{N^{\text{I}2}} - \frac{a_2^{\text{II}}b_1^{\text{II}}c_2}{N^{\text{II}2}} & \frac{a_2^{\text{I}}}{N^{\text{I}}} + \frac{a_2^{\text{II}}}{N^{\text{II}}} - \frac{a_2^{\text{I}}b_2^{\text{I}}c_2}{N^{\text{I}2}} - \frac{a_2^{\text{II}}b_2^{\text{II}}c_2}{N^{\text{II}2}} \end{bmatrix}, \quad (3.2)$$

where  $N^{\text{I}} = 1 + b_1^{\text{I}}c_1 + b_2^{\text{I}}c_2$  and  $N^{\text{II}} = 1 + b_1^{\text{II}}c_1 + b_2^{\text{II}}c_2$  and  $a_i^j = q_{S,i}^j b_i^j$ ,  $i = (1, 2)$ ,  $j = (\text{I}, \text{II})$  in Eq. (2.5). Note that for calculating  $c_2^{M_2^{\text{I}}}$  one has to use  $c_i = c_i^{\text{F}}$  when calculating the partial derivatives given in Eq. (3.2).

Once  $c_2^{M_2^{\text{I}}}$  has been determined, the region of complete separation in Fig. 3.3 follows from the simple expressions given below. For the points  $a$ ,  $b$ ,  $r$ , and  $w$  one finds along the procedure in [117]:

$$m_a^{\text{II}} = a_2^{\text{I}} + a_2^{\text{II}} \quad (3.3a)$$

$$m_a^{\text{III}} = m_a^{\text{II}} \quad (3.3b)$$

$$m_b^{\text{II}} = a_1^{\text{I}} + a_1^{\text{II}} \quad (3.3c)$$

$$m_b^{\text{III}} = m_b^{\text{II}} \quad (3.3d)$$

$$m_r^{\text{II}} = q_{22} \left( 0, c_2^{M_2^{\text{I}}} \right) \quad (3.3e)$$

$$m_r^{III} = m_r^{II} + \frac{q_2(0, c_2^{M'_2}) - m_r^{II} c_2^{M'_2}}{c_2^F} \quad (3.3f)$$

$$m_w^{II} = q_{11}(0, c_2^{M'_2}) \quad (3.3g)$$

$$m_w^{III} = m_w^{II} + \frac{q_2(0, c_2^{M'_2}) - m_w^{II} c_2^{M'_2}}{c_2^F}. \quad (3.3h)$$

For the curved boundaries of the separation regions the following expressions are obtained. Curve *ra* is calculated using  $c_2 = 0 \dots c_2^{M'_2}$  as running parameter and  $m^{II} = m_{\max}^{II}$ :

$$m^{II} = q_{22}(0, c_2), \quad (3.4a)$$

$$m^{III} = m^{II} + \frac{q_2(0, c_2) - m^{II} c_2}{c_2^F}. \quad (3.4b)$$

Curve *wb* is obtained for  $c_2 = 0 \dots c_2^{M'_2}$  in the same way, but here  $m^{II} = m_{\min}^{II}$ :

$$m^{II} = q_{11}(0, c_2), \quad (3.5a)$$

$$m^{III} = m^{II} + \frac{q_2(0, c_2) - m^{II} c_2}{c_2^F}. \quad (3.5b)$$

Finally, curve *wr*, which requires the numerical solution in the rigorous method, is taken as a straight line connecting points *w* and *r*.

It can be seen in the right panel of Fig. 3.3 that for the used parameters the regions of complete separation obtained by the rigorous method (solid lines) and the new shortcut method (dashed) almost coincide. This is due to the basically linear  $\Gamma$  characteristics. The shortcut method from [117] is less accurate (dotted). The latter is based on the simplifying assumption that  $\beta$  lies on a straight line connecting the origin and the feed *F* in the hodograph plane.

Furthermore, Fig. 3.3 (left) shows also concentration profiles obtained by an equilibrium stage model with 1000 stages per zone for the optimal operating points *w* predicted by the three design methods. The shortcut method from [117] (dotted lines) yields purities of 91.787% (raffinate) and 99.901% (extract). The purities obtained such by the shortcut method proposed here (raffinate: 99.579 %, extract: 99.992 %) are only slightly lower than found from the rigorous design (100.0 %, 99.993 %).

In order to critically evaluate the suggested method it is applied to a set of adsorption isotherms that were measured for the enantiomers of mandelic acid on

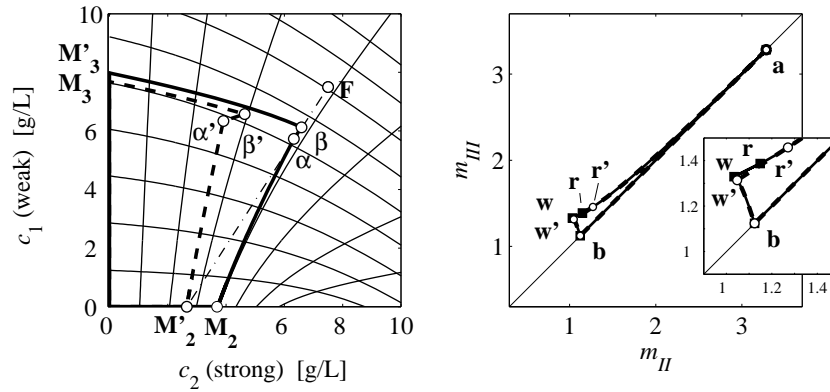


**Figure 3.4** – Application of rigorous and shortcut design method to a set of bi-Langmuir isotherms measured for mandelic acid [137]. Points marked by (') denote the shortcut method. For symbols see Fig. 3.3.

Parameters:  $a_1^I = a_2^I = 1.0366$ ,  $b_1^I = b_2^I = 0.0073$  L/g,  $a_1^{II} = 0.0871$ ,  $a_2^{II} = 2.2461$ ,  $b_1^{II} = 0.0273$  L/g,  $b_2^{II} = 0.7041$  L/g,  $c_1^F = c_2^F = 7.5$  g/L,  $m^I = 1.1$  ( $a_2^I + a_2^{II}$ ),  $m^{IV} = 0.01$ .

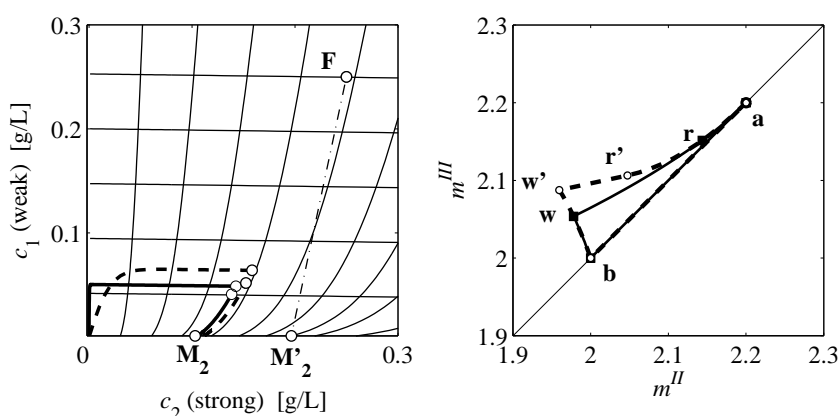
a Chirobiotic T column [137]. As feed concentrations the reported upper validity limits of the isotherms has been applied.

Figure 3.4 (right) shows the determined separation regions. The regions are very narrow, which indicates that the high feed concentration renders the system rather nonlinear. Like in the previous example the differences between both predictions are very small. Since  $w$  and  $w'$  almost coincide, this is also reflected in the purities obtained from the stage model (raffinate: 99.987% from shortcut vs. 99.990%, extract in both cases 100%).

The hodograph representation in Fig. 3.4 (left) reveals curved characteristics for this example. A consequence of this is that the  $\Gamma$  and  $\Sigma$  do not coincide. This is clearly observed for the shocks in zone III that connect the states  $\beta$  to  $M_3$  and  $\beta'$  to  $M'_3$ , respectively. The shocks follow  $\Sigma_-$  paths that are tangent in  $\beta$  and  $\beta'$ , respectively.

Although the obtained separation regions are very similar, the concentration profiles for points  $w$  and  $w'$  determined from the stage model differ significantly. As can be seen in the hodograph plane in Fig. 3.4 (left), the state  $M'_2$  predicted from Eq. (3.1b) (dash-dotted line  $M'_2 - F$ ) is clearly off the  $\Gamma_+$  characteristic that holds for the rigorous design. However, the effect of this on the  $m$ -values in Eqs. (3.3a) through (3.5b) is small, which is why the separation regions are very similar. In view of practical application, the deviations are related to the nonlinearity of the isotherms rather than to the inaccuracy of the method.

As a final example a case is constructed where the  $\Gamma_+$  characteristics are facing upwards. The corresponding results and parameters are given in Fig. 3.5. In this



**Figure 3.5** – Application of rigorous and shortcut design methods to an arbitrary set of bi-Langmuir isotherms with convex upwards  $\Gamma_+$  characteristics. For symbols see Fig. 3.3.

Parameters:  $a_1^I = 0.1$ ,  $a_2^I = a_1^H = 1.9$ ,  $a_2^H = 0.3$ ,  $b_1^I = 0.5\text{L/g}$ ,  $b_2^I = 0.2\text{L/g}$ ,  $b_1^H = 4.0\text{L/g}$ ,  $b_2^H = 0.1\text{L/g}$ ,  $c_1^F = c_2^F = 0.25\text{g/L}$ ,  $m^I = 1.1 (a_2^I + a_2^H)$ ,  $m^{IV} = 0.01$ .

case, the shortcut method yields a too high concentration  $c_2$  for point  $M_2'$ . The separation region found is larger than the correct one. Consequently, Eqs. (3.3g) and (3.3h) yield for point  $w'$  a too low  $m^{II}$  and a too high  $m^{III}$  value, respectively. The purity of the raffinate thus decreases (75.521 vs. 99.351%). The extract remains pure (99.939 vs. 99.993%).

Although the last example uses somewhat extreme parameters which seem not to reflect common practical situations, such scenario seems unfavourable with respect to the shortcut method. However, on the basis of Eq. (2.10) it can easily be verified if such case is at hand, or not.

### 3.3.2 Design for Limited Purity Requirements

Not all applications of SMB chromatography require that the feed mixture is separated completely into the pure components. It is then economically not useful to attain a significantly higher purity than required, because separation costs usually increase exponentially when approaching 100% purity. Also combining an SMB unit with a complementary separation process like crystallization can allow reducing the purity requirements to achieve, in turn, improved overall performance. Such processes are discussed in Section 4.2.

It is generally not trivial to design an SMB process for specific purity requirements lower than 100%. Usually this is done by computationally expensive parametric studies or optimization applied to a mathematical process model. In practi-

cal applications also control schemes can be used. Concerning basic design, only Storti *et al.* [142] reported regions of operating parameters for different outlet purities obtained using equilibrium theory, but under the requirement of complete regeneration of liquid and adsorbent phase in zones *I* and *IV* (for the zone configurations see Figs. 2.2 and 2.4). Under the same requirement Rajendran [143] presented a solution for linear isotherms.

The enclosed manuscript [PII-5] demonstrates for Langmuir isotherms that requiring complete regeneration leads to suboptimal performance and that the optimal operating point can be designed using equilibrium theory.

Parametric studies with an equilibrium stage TMB model revealed that the optimal strategy for Langmuir systems is to control the raffinate purity by allowing a partial breakthrough of the simple wave of the strong adsorbing component from zone *I* to zone *IV*. As shown in Fig. 4 [PII-5] the locus of the optimal operating point in  $(m^{II}, m^{III})$  remains largely unaffected when gradually decreasing  $m^I$ , even if a significant portion of the simple wave migrates into zone *IV*. The attractive aspect is that lowering  $m^I$  or increasing  $m^{IV}$  corresponds to decreasing the desorbent stream. However, increasing  $m^{IV}$  leads to a rapid shrinking of the separation region, see Fig. 5 [PII-5]. A breakthrough of the shock of the weaker adsorbing component from zone *IV* into zone *I* should not be allowed since it causes a drastic decrease of the extract purity. Instead the latter should be controlled by permitting mixed simple waves within both zones *I* and *II*.

These observations were supported by an optimization study performed with the stage model. All four  $m$  values were optimized simultaneously. The results in Fig. 6 [PII-5] underline that this facilitates significantly improved process performance in comparison to requiring complete regeneration.

The concentration profiles for a one of the optimization are shown as an example in Fig. 3.6 (more examples can be found in Fig. 9 [PII-5]). An analysis in the frame of equilibrium theory reveals that this scenario differs from the case of complete separation and regeneration discussed in Sections 2.3 and 3.3.1. The hodograph representation in Fig. 3.6 exhibits several particular features:

- The raffinate  $R$  is located on the intersection of a  $\Sigma_+$ , the  $\Sigma_-$  through  $III$ , and the line defining its purity.
- The state in zone *II* is on the  $\Gamma_+$  characteristic through the feed  $F$ <sup>1</sup>.

<sup>1</sup>In [PII-5] it was stated that the states  $\alpha$  and  $III$  left and right of the feed are “identical”. This is not correct, as can be observed in Fig. 3.6. The states  $\alpha$ ,  $III$  and  $F$  lie on the straight line in the hodograph defined by the material balance around the feed, just as discussed for  $\alpha$ ,  $\beta$  (which is here denoted as  $III$ ) and  $F$  in Section 3.3.1. However, it can be seen from the equations in [PII-5] that this erroneous assumption is *not* used in the design method.

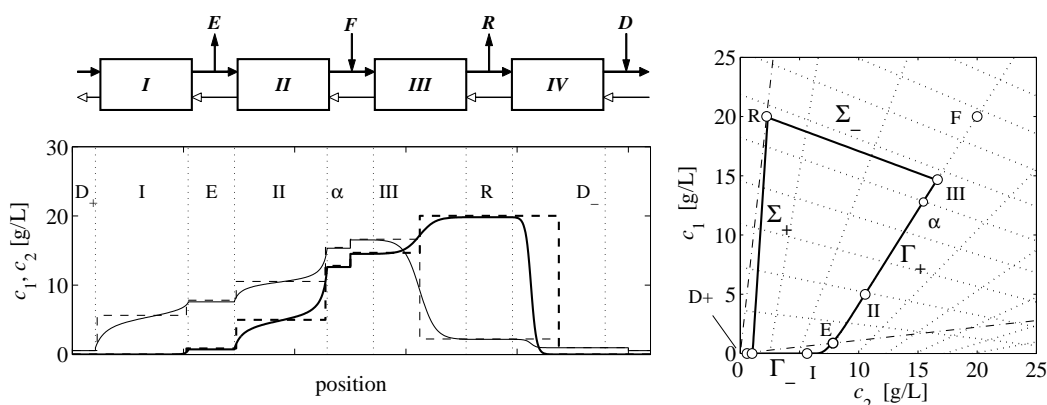


**Figure 3.6** – Concentration profiles obtained from the shortcut design method in comparison to an optimization of all four  $m$  values in a TMB stage model. Raffinate and extract purity equal to 90%. Left – internal concentration profiles, right – hodograph representation. Solid lines – TMB model with 100 stages/zone, dashed – equilibrium theory, thick – weak adsorbing component 1, thick – strong adsorbing component 2, symbols (right) – equilibrium theory, dash-dotted – purity requirements. For parameters see [PII-5].

- The extract  $E$  lies on a boundary discontinuity.
- The state in zone  $I$  is on a  $\Gamma_-$  characteristic with  $c_1 = 0$  and  $c_2 \neq 0$ .

These findings were incorporated into the formulation of the material balances and wave velocities for the process in the frame of equilibrium theory. The resulting set of nonlinear equations can be solved to give the four optimal  $m$  values for a given set of purity requirements. The results shown in Fig. 6 [PII-5] and Fig. 7 [PII-5] match very closely those of the numerical optimization. A simple formulation with only three implicit equations is given in Appendix B of [PII-5].

Finally, it should be mentioned that the proposed method has limitations with respect to the minimal purities that can be applied. The corresponding minimum values are found when the state in zone  $I$  reaches the  $\Gamma_+$  characteristic through  $F$  and/or the state in zone  $II$  reaches the feed composition.

A possible future extension of the approach would be to combine it with the shortcut design method for bi-Langmuir isotherms proposed in Section 3.3.1.

### 3.3.3 Gradients of Adsorbing Additives

Applying adsorbing additives as discussed in Section 3.1 for batch chromatography could also be an interesting strategy in SMB processes. A similar ternary problem was already analyzed in the frame of equilibrium theory in [116]. While

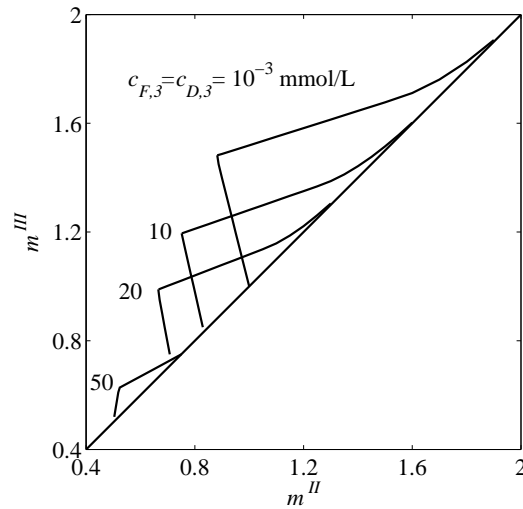


**Figure 3.7** – Regions of complete separation for components 1 and 2 as function of concentration of the additive (component 3) in desorbent and feed. Additive strongest adsorbing.  $c_{F,1} = c_{D,1} = 10$  mmol/L. For isotherm parameters see Fig. 3.1.

there focus was on the conditions for separation in zones *II* and *III*, here the influence of the additive on all zones is discussed.

For illustration the case of the additive being the strongest adsorbing component is considered for a system with Langmuir isotherms. The parameters applied are the same as given in Fig. 3.1, corresponding to the enantiomers of Alprenolol in [PII-4].

For the investigation, the Riemann problem illustrated in Fig. 2.5 in Section 2.3 was solved for all zones of a TMB process together with the mass balances between the zones. Complete regeneration of zones *I* and *IV* from the weakest and intermediate adsorbing components was required.

The resulting set of nonlinear equations was solved in Matlab. Like in Section 3.1 the  $\omega$ -transform [84] is applied because it simplifies the implementation to some extent and facilitates a visual inspection of the solution paths, at least for the ternary problem at hand.

Based on the implementation the regions of complete regeneration can be determined numerically. Figure 3.7 shows selected regions for different additive concentrations adjusted to the same values in the feed and the desorbent streams,  $c_{F,3} = c_{D,3}$ . Similar to the binary case – the region for  $10^{-3}$  mmol/L is basically identical to that found for a binary system from the expressions in [128] – one observes that the separation region shrinks with increasing additive levels, but the

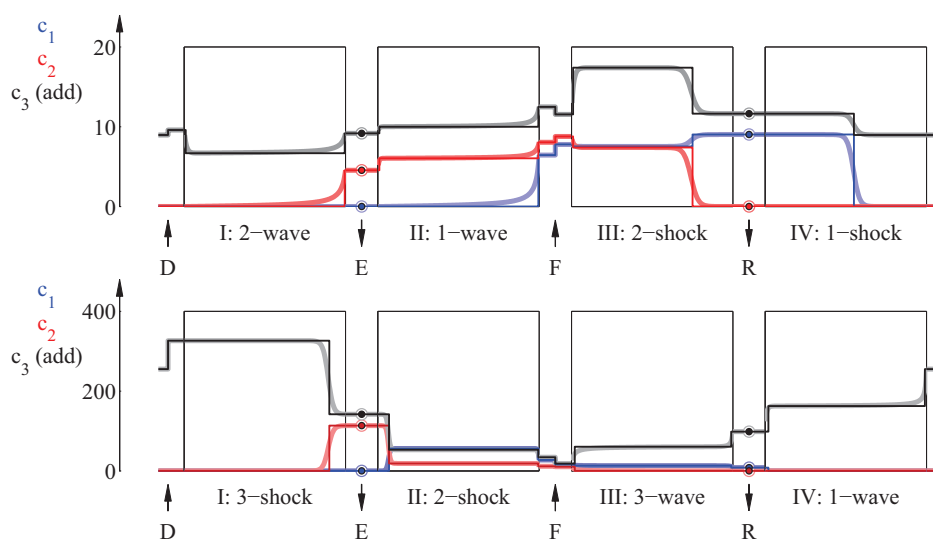


**Figure 3.8** – Change of the type of transition in the zones by changing the additive level in the desorbent. Additive strongest adsorbing. Top – additive concentration  $c_{D,3} = 10$  mmol/L, bottom –  $c_{D,3} = 400$  mmol/L. Feed concentrations  $c_{F,1...3} = 10$  mmol/L. Shaded lines – simulation using a TMB stage model with 10.000 stages. For isotherm parameters see Fig. 3.1. Notation of transitions according to [84].

regions are shifted towards lower  $m$ -values.

At the same time, for increasing  $c_{F,3} = c_{D,3}$  process performance deteriorates in the optimal operating points. In contrast, performance improves with  $c_{F,3} = c_{D,3}$  for the other two enantiomeric systems in [PII-4], where the additive is weakest (Atenolol) or intermediate (Propranolol) adsorbing, respectively.

Using the approach also the possible consequence of an additive gradient can be illustrated. A comparison between the optimal operating points for an isocratic and a gradient case is given in Fig. 3.8. In the former case, where the concentrations are comparable to the experimental conditions used earlier for the Alprenolol system [133], the types of the transitions in the zones – simple waves in zones *I* and *II* and shocks in *III* and *IV* – are the same as familiar from binary separations. On the other hand, the concentration profiles indicate that already this case will pose challenges in practical implementation where exact competitive isotherm parameters are usually not known for such system.

The situation gets more involved when increasing the additive level in the desorbent as in the lower part of Fig. 3.8. Here the types of transitions change for all zones from simple waves to shocks and *vice versa*.

Independent of the last extreme example, gradients of adsorbing additives can result for all cases in an improved performance, independently of the adsorptivity the additive. For a weaker or intermediate adsorbing additive an increased additive level in the desorbent is beneficial. For a strong adsorbing additive a positive effect is obtained only for a very high values of  $c_{D,3}$  that correspond to the situation in the lower panel in Fig. 3.8.

On the other hand, as mentioned for batch chromatography, very high stage numbers are required to take advantage of such gradients. Furthermore, applying high additive concentrations will create additional downstream costs. A detailed study of the possible performance for such systems should thus be performed for industrially relevant conditions.

Apart from that, the observations above underline that in the design of SMB processes that employ an adsorbing additive all four zones should be considered in the design.

### 3.4 Optimal Column Arrangements

At the close of this chapter the optimal arrangement of a set of identical chromatographic columns is addressed. This approach might also be classified into the process combinations treated in the next chapter. However, it is categorized here under “advanced operating modes” because only units of the same type (chromatography) are combine with each other, while the next chapter is reserved to schemes that combine chromatography with unit operations of a different type.

Batch chromatography is still the method of choice for multi-component separations, although also ternary SMB variants were suggested, see *e.g.* [PII-1]. A common situation in industrial practice is that several identical columns are available – for example those in an SMB plant.

An obvious question in such case is how these columns should be arranged in an optimal (batch) process. The enclosed manuscript [PII-6] covers the scenario for using eight identical columns for a ternary separation with an intermediately adsorbing target component. The work extends the binary separation problem with five columns discussed in [14].

A set of eight columns facilitates a significant number of arrangements. A few examples are depicted in Fig. 1<sup>[PII-6]</sup>. Besides 22 possible setups of batch columns in series or parallel, also 6 SMB-batch combinations and 2 SMB/SMB configurations are considered. The different options were evaluated based on the equilibrium-dispersive model by optimizing the operating conditions. These are

injection volume, cycle time and flow rate in batch systems, and (additionally) the  $m$  values for SMB units. The combinatorial complexity could be reduced to a certain extent by a formal evaluation approach for the batch setups. This allows evaluating all 22 options based on the results of only eight optimization runs.

Based on this approach it can be studied how different relevant aspects like feed concentration, particle size or purity requirements affect the optimal arrangement. The main findings are along engineering intuition. The particle size is of particular importance in such problem. Larger particles lead to “longer” arrangements with more columns in series. In turn, there exists an optimal particle size for a given column setup. SMB processes tolerate larger particles. Longer column trains are also required when increasing the purity and/or yield requirements.

For the used parameter set it was found that the batch arrangements outperformed the systems that inherited SMB processes. Simple cascades of standard SMB units were found inappropriate.

Although the results in [PII-6] cannot be generalized, it can be concluded that a flexible multi-column batch system is an interesting option for industrial applications.

# Chapter 4

## Process Combinations

### 4.1 SSR Chromatography with Solvent Removal

Chromatography utilizes a solvent as auxiliary phase. This usually entails an undesired dilution of the products. There are only few exceptions like in displacement chromatography or when collecting a concentrated intermediate plateau caused by competitive adsorption. The dilution is of major economical importance and plays a role for downstream operations. Combinations with, for example, crystallization or with a chemical reaction in a recycle setup (see next sections) usually require an intermediate concentration step.

Applying a partial solvent removal in SMB chromatography has been already proposed in the EE-SMB concept [44, 45]. As concerns SSR chromatography, it can be shown that the dilution of the recycle fraction (*cf.* Fig. 2 <sup>[PII-3]</sup>) worsens the higher the required purity. It is plausible that SSR processes would benefit from reducing this effect by a partial solvent removal.

There exist several options for incorporating such enrichment step in SSR processes. Paper [PII-7] analyses them in the frame of equilibrium theory and proposes a shortcut method for *a priori* design similar to that for ideal systems in Section 3.2.

Figure 4.1 shows the three possible options. Depending on whether the solvent removal is performed for the fresh feed itself (option I), within the recycle stream (II), or directly before the column (III), its operating line in the hodograph representation of the SSR process changes, as demonstrated in Fig. 3 <sup>[PII-7]</sup>.

By extending the design approach for conventional SSR processes under ideal conditions one finds an explicit relation between the amount of fresh feed processable per cycle and the volume of solvent removed, see Eq. (22) in [PII-7]. As a result, in addition to the injection width – which is the only free operating para-

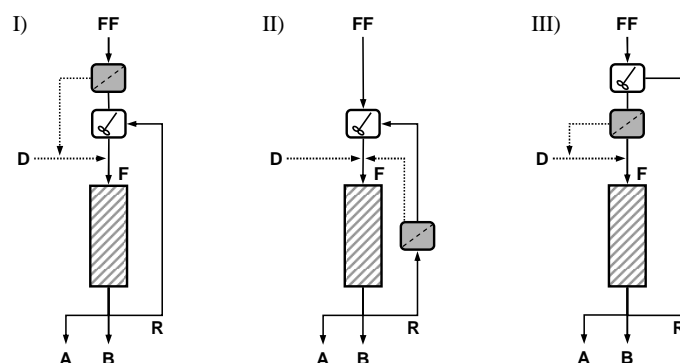


**Figure 4.1** – The different options for performing a solvent removal in SSR chromatography [PII-7]. Setup I – enrichment of the fresh feed, II – enrichment of the recycle fraction, III – enrichment before injection.

meter in conventional SSR processes – also the amount of fresh feed introduced per cycle can be considered a design variable.

The three process options perform identically when operated with the same values for fresh feed volume and total injection width. However, they differ with respect to the feasible regions for adjusting these two parameters as shown in Fig. 5 [PII-7]. The scheme I has a rather restricted operational area. Options II and III can process larger fresh feed amounts. The variant III is the most flexible.

As concerns process performance, an SSR process with solvent removal can outperform batch chromatography in terms of eluent consumption, product concentration as well as productivity. Note that the latter does not hold for conventional SSR processes, see Section 3.2.1. While minimum solvent consumption is achieved in the region above the boundary  $G$  in Fig. 6 [PII-7], the highest productivity is found along the lines  $B$  and  $F$ . These findings are also underlined by the results of a parametric study summarized in Fig. 7 [PII-7].

A future extension of this approach should consider limited solubilities of feed components. These will impose additional boundaries on the operation regions.

## 4.2 Chromatography with Crystallization

A process concept that recently found significant interest is the combination of SMB chromatography and (enantio)selective crystallization [137, 144–148], where an SMB process delivers an only partially separated mixture and the pure product is obtained from a “cheaper” enantioselective crystallization. The approach exploits the fact that the performance of chromatography often improves significantly when lowering the purity requirements. Its overall benefit rises with increa-

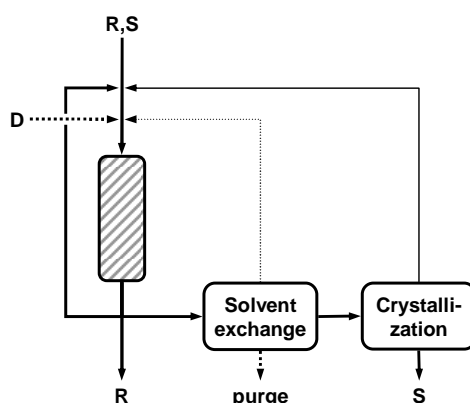


**Figure 4.2** – Combination of chromatography and crystallization for the production of a pure target enantiomer *S* from a racemic mixture. Thin lines denote possible recycles of solvent and mother liquor that were not performed in the experiments.

sing purity demands [137, 146]. Figure 4.2 shows a scheme of the process, which is explained in more detail in Section 7.1 of [PII-1]. Note that usually a solvent removal is required as was discussed in the previous section.

Most of the mentioned investigations of this process combination focus on its laborious optimal design using more or less detailed models. In this context the simple shortcut design methods for SMB and SSR chromatography for limited purity requirements in Sections 3.2 and 3.3.2 are of obvious interest.

Up to now only few experimental studies were published. Below a challenging enantioseparation of an undisclosed pharmaceutical compound is investigated. The scope of the combination is extended to the application of SSR chromatography. Focus of the discussion is on chromatographic aspects.

Producing the desired weaker adsorbing enantiomer of the compound by batch chromatography was not economical, in spite of a separation factor of 1.42 under linear conditions. The reason is a peculiar adsorption behavior. Experiments with pure enantiomers and mixtures indicated a partially collaborative adsorption. Competitive isotherm parameters were determined by applying the inverse method (“peak fitting”) simultaneously to a number of different experimental chromatograms. For a sufficiently accurate modelling the following complex and somewhat empirical isotherm model had to be developed:

$$q_i = \gamma c_i + q_S^I \frac{b_i^I c_i}{1 + \sum_j c_j b_j^I} + q_S^{II} \frac{b_i^{II} c_i + 2b_{q,i} c_i^2 + b_m c_1 c_2}{1 + \sum_k c_k b_k^{II} + \sum_n b_{q,n} c_n^2 + b_m c_1 c_2} \quad (4.1)$$

with  $i = (1,2)$  and  $j,k,n = 1 \dots 2$ . The model assumes linear ( $\gamma$ ), Langmuir-type

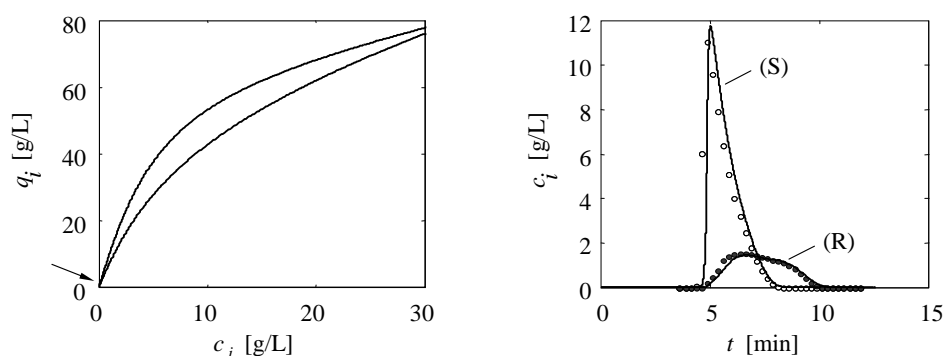


**Figure 4.3** – Left – Competitive adsorption isotherms for the pharmaceutical component for  $c_R = c_S$ . The arrow indicates the concentration range where an inflection point occurs in the isotherm of the stronger retained species. Right – Model validation. Experiment (symbols) and simulated (lines) results for the injection of an asymmetric mixture.

Parameters. Isotherms, Eq. (4.1):  $\gamma = 0.6331$ ,  $q_S^I = 64.7$  g/L,  $b_1^I = 0.0316$  L/g,  $b_2^I = 0$ ,  $q_S^{II} = 46.8$  g/L,  $b_1^{II} = 0.1035$  L/g,  $b_2^{II} = 0.2056$  L/g,  $b_{q,1} = 0.0056$  L<sup>2</sup>/g<sup>2</sup>,  $b_{q,2} = 0.0258$  L<sup>2</sup>/g<sup>2</sup>,  $b_m = 0.0188$  L<sup>2</sup>/g<sup>2</sup>. Experiment:  $c_{inj} = 20$  g/L (total, S:R = 3:1),  $V_{inj} = 2$  mL, 2 mL/min.

(I) and competitive-collaborative adsorption on another adsorption site (II). Regarding the latter, interactions between the same species ( $b_{q,i}$ ) and among the two enantiomers ( $b_m$ ) are considered. Figure 4.3 shows the isotherms and one of the experiments performed to validate the used transport-dispersive model.

Despite the existence of an inflection “point” in the isotherm of the stronger adsorbing  $R$  at, for example,  $c_R = 0.53$  g/L for  $c_S = 0$  and at  $c_S = c_R = 0.22$  g/L, the tail of the second component remains sufficiently constant over a wide range of injection parameters. Therefore the shortcut design method for SSR chromatography under nonideal conditions described in Section 3.2.2 could be applied to investigate the possible performance of an SSR process.

Figure 4.4 shows the obtained results for the a “symmetrical” purity requirement of 95% for both fractions, which was identified as suitable operating point. Note that in this case the optimal performance is not achieved by maximizing the feed concentration, but for an intermediate value of about  $c_S = c_R = 12.5$  g/L. The figure reveals that the SSR process achieves a significantly better performance than a batch separation. Productivity is about 120% higher and solvent consumption 57% lower, respectively. The product concentrations (not shown) increase by 222% and 93%, respectively.

The mentioned operating point was then applied in an SSR experiment using an analytical column and the experimental setup in Fig. 3.2. The process was successfully started into immediate steady state by the procedure described in

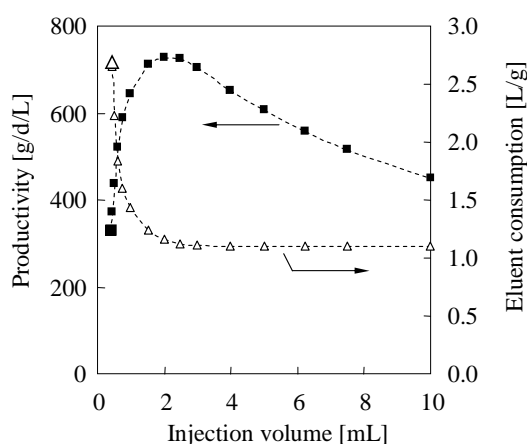


**Figure 4.4** – Predicted performance of SSR chromatography as function of the injection volume for the pharmaceutical compound. Calculated using the shortcut method for nonideal systems in Section 3.2.2 for a purity of 95% for both fractions and an injection concentration of 25 g/L (rac.). Enlarged symbols mark the optimal operating point of batch chromatography when requiring the same yield and purity.

Section 3.2.2. After a total of 126 cycles (16 hours), 775 mL of the first product fraction were obtained with a purity of 93.4% (design value: 95%). This corresponds to a productivity of about 270 g/d/L. This is lower than the possible 730 g/d/L indicated in Fig. 4.4 because strict safety margins were applied between the cycles.

From the collected solution a total of 470 mg solid (S)-enantiomer was crystallized in enantiomerically pure form, which corresponds to a yield of 54%. Note that a rather conservative procedure was applied at this initial stage in order to keep a sufficient distance to the eutectic composition at 67%.<sup>1</sup>

The promising results of these initial experiments motivated the investigation of the more advanced process concept covered in the next section, where not only the recycle of the mother liquor (thin lines in Fig. 4.2) was practically implemented, but additionally a racemization of the (R)-enantiomer was performed to improve the overall yield.

## 4.3 Chromatography with Isomerization Reactions

The separation processes considered so far split a feed mixture into two fractions that fulfill given purity requirements. However, often only one of the components

<sup>1</sup>The author gratefully acknowledges the help of Dr. Jan von Langermann, Max Planck Institute Magdeburg, Germany, who performed the crystallization.

is desired as product while the others are of no particular interest. This is particularly true in enantioseparations, since typically only one of the enantiomers has the desired physiological effect.

The production and subsequent separation of a 50/50 mixture of two enantiomers, which is a common industrial practice, therefore inherently limits the possible overall yield to 50% only. For a number of compounds this can be overcome by devising a combining of the (chromatographic) separation with an isomerization of the undesired enantiomer. The latter is denoted as racemization, and occurs in some cases spontaneously. It can also be triggered (bio)catalytically, under basic or, less frequently, acidic conditions.

The conventional approach for a corresponding process is to perform a racemization at the outlet of the undesired species and to recycle the racemized solution back to the inlet of the separation process. Such processes are discussed in [149–152] and [PII-9], [PII-10].

Besides the few mentioned theoretical works there is a lack of experimental results that would demonstrate a coupling of these unit operations with an actually closed recycle. An attempt in this direction was made by the author for the spontaneously racemizing enantiomers of Chlorthalidone by combining an SSR process with a homogeneous racemization in a heated vessel [152]. However, a reasonable steady state was not reached due to a strongly diluted recycle. A partial solvent removal would be required there.

Here the case study for the pharmaceutical compound from the previous section is continued for a combination of batch chromatography and a homogeneous catalytic racemization of the (R)-enantiomer. The concept is further extended by also including the enantioselective crystallization step discussed in the previous section. Again, focus will be on chromatographic aspects.

Figure 4.5 shows the complete flowsheet for this process. The racemization is performed here using a homogeneous catalyst. It can be seen that besides the three main units chromatography, crystallization and racemization also several solvent-related operations are performed. These are performed mainly to withdraw eluent components that are not compatible with the conditions required for crystallization or racemization. An interesting aspect is that the racemization is actually concluded by another crystallization step (not shown) in order to separate the racemate from the homogeneous catalyst.

The concept was validated experimentally at preparative scale by an industrial partner. For an optimal design the following main parameters have to be specified: flow rate, injection volume, and injection concentration in chromatography;

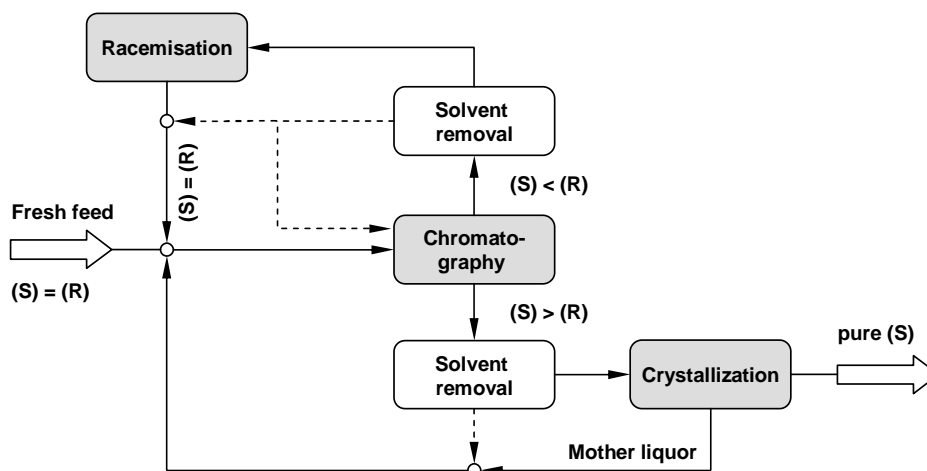


**Figure 4.5** – Process combination of chromatography, enantioselective crystallization and racemization for the production of a single pure enantiomer at a yield of 100%.

coupling purity between chromatography and crystallization, coupling purity between chromatography and racemization, and final purity of the mother liquor in crystallization.

The flow rate was determined as 236 mL/min in a conventional scale up from the analytical 25 x 0.46 cm column used in Section 4.2 to a given 25 x 5 cm column by keeping constant the interstitial velocity. The purity of the mother liquor was specified to 75% to guarantee a safety margin to the eutectic of 67%.

An initial optimization for the remaining parameters using a conventional simplex algorithm [153] in MATLAB minimizing the ratio of productivity and eluent consumption showed poor convergence. This appears related to the simultaneous optimization of injection volume and feed concentration. Since it is known that concentration overloading is usually superior to volume overloading [154], it could be better to replace the two variables by the injected amount.

Since here it was also of interest to confirm the intermediate feed concentration found optimal for the SSR experiments in Section 4.2. Thus, a dense “scanning” of the operating parameters was performed. The optimal values found are an injection volume of 180 mL, racemic injection concentration of 24 g/L (similar to Section 4.2), a coupling purity to crystallization of 89 %, and a coupling purity to racemization of 76 %.

These operating parameters lead to an adequate overall process performance with a productivity of 469 g/d/L and a solvent consumption of 1.56 L/g. Most importantly, the process achieves an overall yield of 99.8%<sup>2</sup>.

<sup>2</sup>The missing 0.2% are due to the fractionation strategy in chromatography that is based on

Based on this design the process was implemented and tested by an industrial partner [155–157]. Several cycles were performed where each processing step was performed batch-wise and the process was found sufficiently stable. This is considered as a successful validation of the concept.

Before concluding, it is interesting to note that in the optimal operating point both streams from chromatography have limited purity. This underlines again the usefulness of the corresponding design methods for SMB and SSR chromatography in Chapter 3. The methods can be extended for the process combination above by determining the feed composition for chromatography through corresponding mass balances.

Finally, the task of maximizing the yield by including an isomerization can also be accomplished by the reactive SMB processes expounded in Chapter 5.

## 4.4 Optimal Synthesis of Process Combinations

The case study in the previous sections illustrates that a number of competing process alternatives exist for producing a single enantiomer. Already when considering the possible combinations of an SMB unit with selective crystallization immediately four possible schemes are recognized: stand-alone chromatography, a single crystallizer at either one of the two outlets, or two at both outlets [146]. Taking into account also racemization, solvent removal, re-crystallization, purge streams, etc. it becomes evident that identifying all options is already tedious, let alone deciding on the optimal one.

In conventional process synthesis all useful process candidates are identified at first, then designed on the basis of suitable models, and finally evaluated against each other. Often this must be repeated if a different substance should be produced, because the economically optimal setup depends on process requirements, properties of the substance, operational constraints and cost factors.

An interesting alternative is to formulate this task as a mixed-integer nonlinear programming (MINLP) problem. This allows finding the optimal process by simultaneously optimizing the structure and the operating parameters. The approach is based on defining a suitable superstructure that inherits all useful process alternatives. Integer numbers with a value of either zero or unity serve as structural decision variables specifying the existence of a unit or stream. Operating parame-

---

threshold concentrations.

ters are continuous variables. This approach is well-known in particular for the synthesis of distillation sequences and heat exchanger networks [158–160].

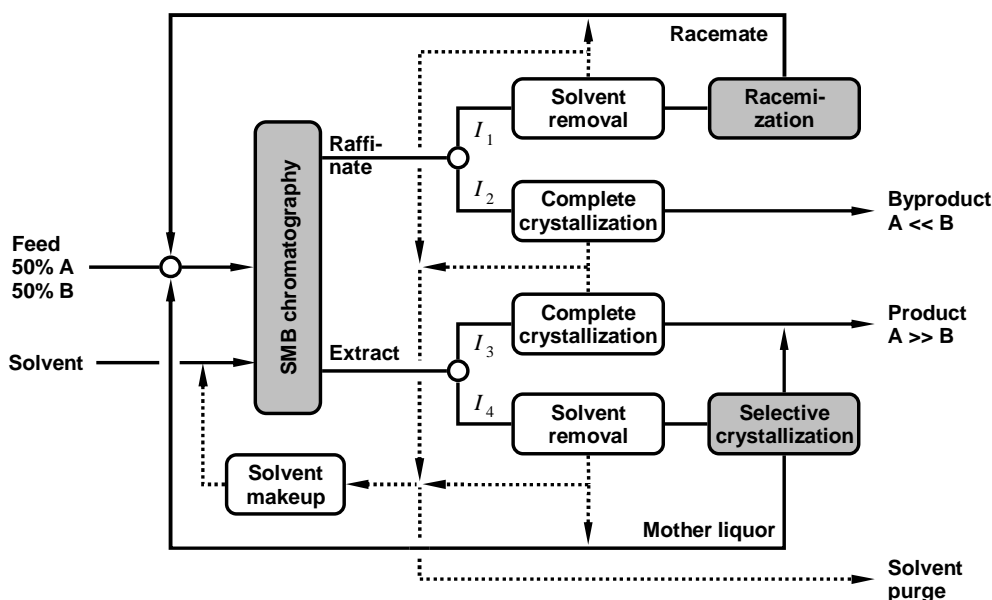


**Figure 4.6** – Superstructure for the determination of an optimal process for the production of a stronger adsorbed enantiomer A from a racemic mixture.

Here this approach was extended to design process combinations for enantioseparations that inherit SMB chromatography. The problem was formulated in the modeling environment GAMS using a similar as in [161]. Figure 4.6 shows an example of an according superstructure. The SMB process is approximated by a steady-state equilibrium stage TMB model. Other units are modeled as simple splitters or mixers.

The integer variables  $I_j \in \{0, 1\}$ ,  $j = 1 \dots 4$  are multiplied with the flow rates at the indicated positions. As constraints it is required that  $I_1 + I_2 = 1$  and  $I_3 + I_4 = 1$ . This renders possible four different “trains” at the two SMB outlets. They can represent product ports ( $I_1 = 0, I_2 = 1$ ) and ( $I_3 = 1, I_4 = 0$ ), connected to the crystallizer ( $I_3 = 0, I_4 = 1$ ), or sent to racemization ( $I_1 = 1, I_2 = 0$ ), respectively.

The MINLP problem is solved in GAMS using SBB, a standard branch and bound method, in connection with the multi-method NLP solver CONOPT.

Different scenarios were investigated [157] minimizing cost functions of different degree of detail. Each of the inherited sub-structures can be identified as optimum, depending on the definition of the various possible cost factors and constraints on purity, yield, eutectic composition, etc.

Before concluding this section a few remarks seem useful. In principle the two trains defined by  $I_3$  and  $I_4$  in Fig. 4.6 could be replaced by a single crystallizer with a recycle ratio as NLP variable. However, a complete crystallization with total solvent removal has a different scope and cost function than a selective crystallization.

A limitation of this approach is related to the selective crystallization. To fully exploit the potential of such process combination, an optimum balance between column efficiency and pressure drop has to be found for the SMB process [137, 147]. A scale-up procedure based on a pressure drop relation and the van-Deemter equation as in [137, 146] was implemented. Yet, a reliable method for matching the dispersion between TMB and SMB models is lacking, which limits the accuracy of the predictions. A detailed design requires optimization using an SMB model as applied in [147]. A viable option seems also extending the MINLP approach in [63, 162, 163] into this direction.

Apart from such approaches for detailed design, the method illustrated above can serve as a valuable tool for a basic initial design of corresponding flowsheets.

# Chapter 5

## Integrated Reactive Processes

Reactive chromatographic processes combine a chemical reaction and the chromatographic separation of the products into a single apparatus, usually with the goal of improving the conversion for equilibrium-limited reactions.

Reactive chromatography has been studied intensively for batch and SMB chromatography in particular for reversible reactions with stoichiometries of  $A \rightleftharpoons B + C$  and  $A + B \rightleftharpoons C + D$ , see *e.g.* [15, 17–23, 82, 83, 85, 164]. The majority of publications investigates esterifications, ester hydrolyses and transesterifications due to the favourable adsorptivity of the components and the catalytic activity of the used stationary phases.

In the following the focus is on aspects and concepts less frequently considered in reactive chromatography. Section 5.1 studies the role of temperature effects in reactive liquid chromatography. In Section 5.2 investigates the possible integration of SMB chromatography and isomerization reactions. The according stoichiometry  $A \rightleftharpoons B$  has rarely been considered for difficult applications like the production of a pure enantiomers from racemates discussed in Chapter 4.

### 5.1 Thermal Effects in Reactive Chromatography

Thermal effects are usually neglected in non-reactive liquid chromatography by assuming that heats of adsorption are negligible in comparison to the heat transport by the eluent. It will be elucidated below that in non-isothermal reactive liquid chromatography heat effects due to adsorption and reaction should be taken into account.

These aspects are investigated experimentally and theoretically in the enclosed manuscript [PII-8]. The studied model reaction is the esterification of methanol

with acetic acid performed at ambient temperature in a thermally insulated semi-preparative column of 47.5 x 2.6 cm, equipped with six thermocouples along the bed. The reaction is catalyzed by the stationary phase, an acidic cation exchanger in  $H^+$  form. The heat of this weakly exothermic reaction is  $\Delta_r H = -4.6$  kJ/mol, which is in the order of typical heats of adsorption, at least for reversed-phase chromatography [165].

Fig. 2 [PII-8] shows for a frontal analysis experiment that a moving, self-amplifying thermal wave develops in the column under adiabatic conditions. The overall temperature change is about  $+5$  K, but a maximum temperature increase of  $20$  K is observed. This is significant and needs to be accounted for when aiming at detailed process modeling.

When performing non-reactive frontal analysis by replacing water from the column with 94% ethanol as shown in Fig. 3 [PII-8], significant effects can also be observed. The endothermic desorption of water causes a sharp negative temperature change, which is almost completely cancelled out by the exothermic mixing of ethanol and water. Finally, when switching to pure ethanol after 50 min, a broad negative temperature response appears. This is caused by the displacement of the strongest adsorbed water molecules.

It is obvious that such temperature waves must affect process performance. Although not applied here, it is worthwhile considering the propagation velocities of concentration wave,  $u_c$ , and that of a thermal wave,  $u_T$ , as given by equilibrium theory for non-reactive chromatography [84]:

$$u_c = \frac{u}{1 + F \frac{\partial q}{\partial c}}, \quad (5.1)$$

$$u_T = \frac{u}{1 + F \frac{\rho_s c_{p,s}}{\partial \rho_l c_{p,l}}}. \quad (5.2)$$

The analogy is obvious. The velocity of the temperature wave is controlled by the ratio of the heat capacities in Eq. (5.2). Furthermore, it is known that these velocities are coupled through the enthalpies of adsorption. This facilitates an analysis based on reduced variables that represent energy contents [84]. In [PII-8] an analogous approach was used to define the equations of a more detailed model of the reactive problem without having to consider an energy balance.

A numerical study using this model demonstrates that the development of the thermal waves can have beneficial effects. As shown in the elution and temperature profiles in Fig. 4 [PII-8], self-sharpening fronts can develop even for linear

isotherms. On the other hand, also severe tailing is observed towards the end of the elution.

Despite the latter, the thermal waves can improve productivity and conversion in such systems, as shown in Fig. 6 [PII-8]. The main parameter that controls the performance is the mentioned heat capacity ratio in Eq. (5.2).

These results underline that a non-isothermal operation, although it increases the complexity in modeling and design, represents an interesting concept for reactive chromatography.

## 5.2 Integrated SMB Processes for Equilibrium-limited Isomerization Reactions

Process concepts applying reactive SMB chromatography to equilibrium-limited isomerization reactions could be interesting alternatives to the conventional reactor-separator processes discussed in Section 4.3. However, they have been studied mainly in the context of obtaining products with limited purity as, for example, in the interconversion of sucrose and fructose. Only few works investigate the production of compounds with high purity as required when producing enantiomers. More details on the existing literature can be found in the introductions of [PII-9] and [PII-10].

The reason for the lack of processes for this type of problem is the stoichiometry  $A \rightleftharpoons B$  of reversible isomerizations. A simultaneous occurrence of reaction and separation prohibits here obtaining a pure compound at sufficient productivity. As a consequence the functionalities “reaction” and “separation” should be distributed spatially along the chromatographic process. This can be achieved by using side reactors as proposed by Hashimoto [75]. However, as will be shown, side reactors are of limited use when aiming at high product purity.

Below the results of a systematic development of corresponding integrated SMB processes are summarized. Although focus is on producing single enantiomers, it is emphasized that most results are generally valid and can be applied directly to other isomerization problems.

### 5.2.1 Conceptual Process Development

In a first step, simple TMB models are applied to gain insight into the general behavior and specific requirements on reactive SMB processes with an integrated

racemization.

For this purpose, the three general concepts for process integration shown in Fig. 1 [PII-9] are considered. These are conventional reactor-separator-recycle processes, processes with side reactors, and reactive chromatographic processes (in the following also denoted as “fully integrated”). Based on these concepts, the five processes shown in Fig. 2 [PII-9] can be defined, the first of which reflecting the idea pursued in Section 4.3. The author published first results in this direction for the enantiomers of Chlorthalidone [152].

The performance in terms of the specific eluent consumption is maximized for each scheme using the parameters from [152]. Optimized variables are the  $m$ -values in the individual zones as well as the Damköhler numbers in the zones of the integrated processes 4 and 5 in Fig. 2 [PII-9]. This allows creating an optimal spatial distribution of the reaction functionality within these units.

The results in Tables 2 and 3 in [PII-9] can be summarized as follows. The best performance will be achieved by a fully integrated process that utilizes chromatographic reactors with a reaction rate “adjustable” to different values in the individual zones. The reaction should preferably be restricted to the regeneration zone. Furthermore, the achievable benefit increases for the integrated systems with increasing purity requirements, increasing separation factor, and for more favourable reaction equilibria.

The superior performance of these (hypothetical) processes is due to an effect denoted as reaction-assisted regeneration. This means that performing the reaction in the regeneration zone actually facilitates there an easier regeneration of the solid or the fluid phase. This is seen when inspecting the determined  $m$ -values. If the weaker adsorbing enantiomer is produced (Tab. 2 [PII-9]), in the reactive zone  $I$  of processes 4 and 5 significantly lower  $m$ -values suffice for regeneration than required in the non-reactive SMB unit of process 1. Similarly,  $m^{III}$  and  $m^{IV}$  are higher when the stronger adsorbing species is obtained (Tab. 3 [PII-9]). The data reveal also that this effect is less pronounced for the Hashimoto process.

The  $m$ -values actually required for completely regenerating a reactive zone can be determined from equilibrium theory by introducing transformed concentration variables. The necessary values for the case of Langmuir isotherms are tabulated in the manuscript for homogeneous and heterogeneous reactions. Fig. 2 [PII-9] shows them for the mentioned zone  $I$ .

A more detailed elucidation of this effect for bi-Langmuir isotherms will be given in Section 5.2.3 together with a design method derived from equilibrium theory for the 3-zone processes.

### 5.2.2 Optimization-based Synthesis of SMB Processes

In view of the limitations of TMB models and practical implementation, the analysis above is extended in [PII-10] to more realistic SMB processes. In SMB units the existence of several columns in each zone corresponds to having more structural options. A generation of the possible process variants is, thus, more difficult than for the TMB processes considered so far. Therefore here an MINLP approach is applied to simultaneously optimize process setup and conditions. However, due to the periodic nature of SMB processes this is more difficult than for the flowsheets optimization discussed in Section 4.4.

In order to cope with this the five different superstructures shown in Fig. 1 [PII-10] and Fig. 2 [PII-10] were defined that reflect the different concepts for process integration already illustrated in Fig. 1 [PII-9]. The structures inherit a total of 130 possible setups. The models were formulated in the simulation environment DIVA, and the MINLP problem was solved using an evolutionary algorithm.

The trends observed earlier for TMB processes were confirmed in a first step by assuming idealized conditions with established reaction equilibrium and negligible size of side reactors. The fully integrated processes with four and three zones, numbered as 3 and 5 in [PII-10], achieve a better performance than the conventional reactor-separator scheme (1) and the Hashimoto concepts (2 and 4), see Tables 1 and 2 in [PII-10].

These differences increase under more realistic conditions with a limited reaction rate and finite holdup of side reactors. The Hashimoto concept is clearly outperformed by the fully integrated processes, in particular when producing the weaker adsorbing component, see Tab. 4 [PII-10]. A large number of columns and side reactors would be required, see Fig. 4 [PII-10], which in turn limits throughput. Furthermore, the holdup of these reactors necessitates higher flow rates for column regeneration as illustrated in Fig. 5 [PII-10].

The developed three-zone process (5) in Figs. 1 and 2 in [PII-10] appears particularly interesting not only due to its good overall performance, but also for its simple structure without a unit for solvent removal. As discussed earlier, such solvent removal is indeed beneficial, but difficult to implement in practice.

A detailed study of this process demonstrates that it should be capable of producing a pure enantiomer from a racemic mixture. As shown in Fig. 7 [PII-10], the most influential parameter for this process is the adjustable ratio of the reaction rates in the zones responsible for chemical conversion and that in the separation zones, respectively.

As concerns a practical implementation, it is expected that a corresponding ratio can be adjusted in an SMB process by applying a suitable gradient that affects the

reaction kinetics. Envisaged options are gradients of the temperature, pH value, homogeneous catalysts, enzymes, inhibitors, and solvents.

A systematic scanning of the parameter space for the 3-zone process proposed in Section 5.2.2 reveals that there exist, in analogy to the “triangle theory” for non-reactive SMB processes, regions of feasible operating parameters for the  $m$ -values. These are shown as functions of the purity requirements and the mentioned reaction rate ratio in Fig. 6<sup>[PII-10]</sup> and Fig. 8<sup>[PII-10]</sup>.

In summary the studies above revealed several interesting ideas for integrated SMB processes that can be applied to isomerization problems. A developed simple three zone process is of particular interest. The following two sections are devoted to the simplified design of this concept and its experimental validation, respectively.

### 5.2.3 Design Method for a Developed 3-zone Process

The results obtained above for the integrated SMB process with three zones motivate a more detailed investigation. Here in particular the question is addressed whether the separation region shown in Fig. 8<sup>[PII-10]</sup> can be determined.

As discussed above the improved performance of the integrated processes stems from the easier regeneration facilitated by the reaction. An analysis in the frame of equilibrium theory for the case of Langmuir isotherms is given in [PII-9].

This analysis is extended here to the bi-Langmuir model. The results are used to derive a design method for the 3-zone processes above that hold in all cases of interest, that is, independently of the desired product, type of reaction (homogeneous or heterogeneous), and for both Langmuir and bi-Langmuir isotherms.

For the sake of brevity mathematical details will be published elsewhere [166].

#### Required $m$ -values for complete regeneration

The problem to be solved is to calculate the optimal  $m$ -values that completely regenerate a zone in which the isomerization reaction occurs. That is, for process 5 in Fig. 1<sup>[PII-10]</sup> the minimum value of  $m^I$  is desired that displaces the simple wave from this zone (denotes as  $m_w$  below). Analogously, for process 5 in Fig. 2<sup>[PII-10]</sup> the maximum value of  $m^{III}$  is sought for that guarantees that the shock remains stationary in this zone (denoted as  $m_s$ ).

This problem is studied first numerically for single zones for both scenarios. Figure 5.1 shows the corresponding Riemann problems together with the  $m$ -values

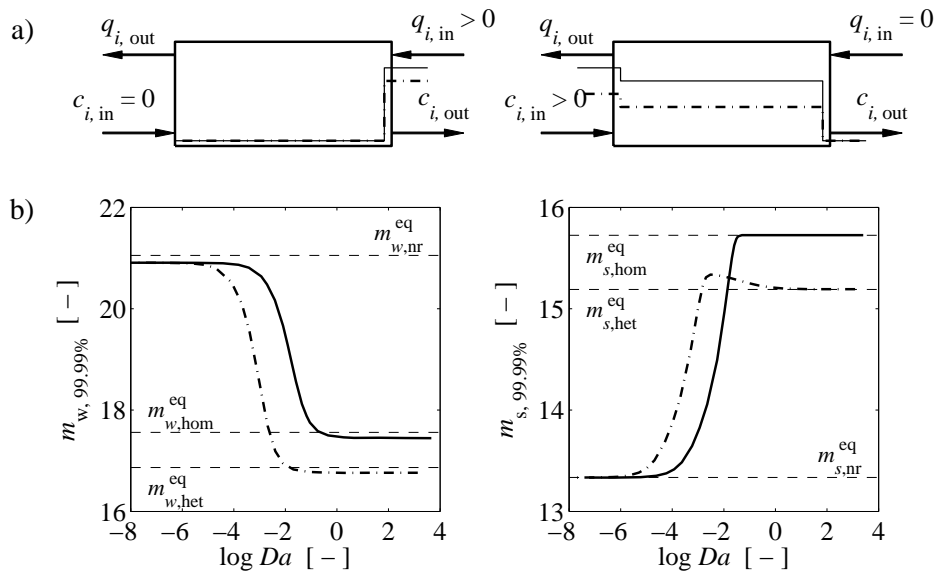


**Figure 5.1** – Regeneration of single TMB zones for bi-Langmuir isotherms in the presence of an isomerization reaction. Left – regeneration of solid for a simple wave, achieved if  $q_{i,out} = 0$ . Right – regeneration of fluid for a shock, achieved if  $c_{i,out} = 0$ . a) Riemann problems considered. b)  $m$ -values required for 99.99% regeneration obtained numerically for above scenarios as function of  $Da$  for homogeneous (solid lines) and heterogeneous (dashed) reaction. Dashed lines mark the solutions from equilibrium theory (superscript eq) given in Table 5.1 below. Subscripts eq,nr,hom,hets denote equilibrium theory, non-reactive case, homogeneous and heterogeneous reaction, respectively.

Parameters: 500 equilibrium stages, reaction rate constant  $k = 10^5 \text{ min}^{-1}$ , other in [PII-10].

**Table 5.1** – Optimal  $m$ -values for complete regeneration of reactive zones for simultaneously established reaction and adsorption equilibria. The case of Langmuir isotherms is included for  $H_{i,2} = 0$ .

	Regeneration of fluid for simple wave, $m_w$	Regeneration of solid for shock, $m_s$
Non- reactive case	$\sum_{i=1}^2 H_{A,i}$	$\sum_{i=1}^2 \frac{H_{B,i}}{1 + b_{B,i}C_B}, (c_A = 0)$
Homo- geneous reaction	$\sum_{i=1}^2 \frac{H_{A,i} + H_{B,i}K_{eq}}{1 + K_{eq}}$	$\sum_{i=1}^2 \frac{H_{A,i} + H_{B,i}K_{eq}}{1 + K_{eq} + (b_{A,i} + b_{B,i}K_{eq})C}$
Hetero- geneous reaction	$\frac{(1 + K'_{eq})(H_{A,1} + H_{A,2})(H_{B,1} + H_{B,2})}{K'_{eq}(H_{A,1} + H_{A,2}) + (H_{B,1} + H_{B,2})}$	$\frac{1 + K'_{eq}}{2K'_{eq}} [K'_{eq} q_A/C + q_B/C]$

that achieve complete regeneration as function of the Damköhler number,  $Da$ , for both types of reactions. The effect of the reaction-assisted regeneration discussed earlier is clearly observed. Furthermore, the results are very close to the values predicted by equilibrium theory to be discussed next.

An analysis of the scenarios in Fig. 5.1 a) is possible by introducing transformed concentration variables that take into account the simultaneous reaction and adsorption equilibrium. These transform the mass balances of the reactive case, which is a set of heterogeneous PDEs, into a homogeneous PDE system [85, 167]. This can be solved by the conventional solution strategies of equilibrium theory, as demonstrated in [PII-9] for the case of Langmuir isotherms. This treatment is extended here to the bi-Langmuir model<sup>1</sup>.

For the reversible isomerization reaction  $A \rightleftharpoons B$  one can define for the fluid and

<sup>1</sup>The author is grateful to J. G. Palacios and D. Flockerzi who performed the derivation of the  $m$ -values for complete regeneration reported here.

the solid phase,<sup>2</sup>

$$C = c_A + c_B, \quad (5.3)$$

$$Q = q_A + q_B. \quad (5.4)$$

For the two desired  $m$ -values then holds in analogy to a non-reactive separation,

$$m_w = \left. \frac{dQ(C)}{dC} \right|_{C=0}, \quad (5.5)$$

$$m_s = \frac{Q(C)}{C}. \quad (5.6)$$

To calculate the  $m$ -values from these equations, explicit expressions of the transformed equilibrium function  $Q(C)$  will be useful. These can be found by deriving corresponding relations for  $c_i(C)$ , as shown below.

For a *homogeneous* reaction,

$$K_{eq} = \frac{c_B}{c_A}, \quad (5.7)$$

one finds from Eq. (5.3)

$$c_A = \frac{1}{1 + K_{eq}} C, \quad (5.8a)$$

$$c_B = \frac{K_{eq}}{1 + K_{eq}} C. \quad (5.8b)$$

For a *heterogeneous* reaction with an reaction equilibrium given by

$$K'_{eq} = \frac{q_B}{q_A}, \quad (5.9)$$

one finds by a more involved derivation from Eq. (5.9) and Eq. (5.9) a quadratic relation between  $c_A$  and  $C$ :

$$A_2 c_A^2 - 2A_1(C) c_A + A_0(C) \stackrel{!}{=} 0, \quad (5.10)$$

$$\text{with} \quad (5.11)$$

$$A_2 = K'_{eq}(a_{12} - a_{11}) + (a_{22} + a_{21}),$$

$$A_1 = \frac{1}{2} [(K'_{eq}\gamma_1 + \gamma_2) + (K'_{eq}a_{12} - a_{21} + 2a_{22})C],$$

$$A_0 = C(\gamma_2 + a_{22}C),$$

$$\gamma_1 = H_{A,1} + H_{A,2}, \gamma_2 = H_{B,1} + H_{B,2},$$

<sup>2</sup>For the sake of simplicity the notation in [PII-10] is applied. Species  $A$  is stronger adsorbing than  $B$ ,  $i = 1, 2$  correspond to the two terms  $I$  and  $II$  of the bi-Langmuir model, Eq. (2.5).

$$\begin{aligned} a_{11} &= H_{A,1}b_{A,2} + H_{A,2}b_{A,1}, a_{12} = H_{A,1}b_{B,2} + H_{A,2}b_{B,1}, \\ a_{21} &= H_{B,1}b_{B,2} + H_{B,2}b_{B,1}, a_{22} = H_{B,1}b_{A,2} + H_{B,2}b_{A,1}. \end{aligned}$$

For the isotherm parameters from [152] studied here,  $A_2$  turns out to be non-negative, which leads to

$$c_A = \frac{A_0(C)}{A_1(C) + \sqrt{[A_1^2(C) - A_2A_0(C)]}}. \quad (5.12)$$

Equations (5.8) and (5.12) can now be substituted into the bi-Langmuir isotherms, Eq. (2.5). From the calculated loadings  $q_i$ ,  $Q(C)$  is calculated from Eq. (5.4) and, finally, the desired  $m$ -values from Eqs. (5.5) and (5.6).

Table 5.1 summarizes the resulting expressions for the minimum  $m_w$  and maximum  $m_s$  for homogeneous and heterogeneous reactions.

### Design method

The expressions in Table 5.1 are valuable for deriving a design method for the reactive 3-zone processes, since they readily specify the optimal  $m$ -values in the regeneration zones under the requirement case of complete separation. On this basis it is possible to establish regions of complete separation for the remaining two zones of each process configuration.

However, the reactive zones under investigation here require a special consideration. In an SMB system the concentration profiles are moving periodically into and out of a reactive zone, which facilitates a complete conversion of the undesired species and simultaneously a complete regeneration of this zone. However, this is a contradiction in the context of TMB processes, since there a completely regenerated zone would have no capacity for the reaction to take place.

This conflict is resolved by introducing the concept of a *reactive boundary*. This means that the components transported towards a reactive zone are immediately converted once they reach the boundary of the zone. Thus, the liquid (solid) leaving this boundary is in reaction equilibrium with the entering solid (liquid). The reaction takes place in the zone either right or left of the feed node. Thus, introducing the concept of the reactive boundary allows determining the states left and right of the feed node for each process configuration. The region of complete separation is then found along the lines of the shortcut design method for non-reactive SMB processes explained in Section 3.3.1. The problem is formulated implicitly with the concentrations of the two components either left or right of the feed state as unknowns.

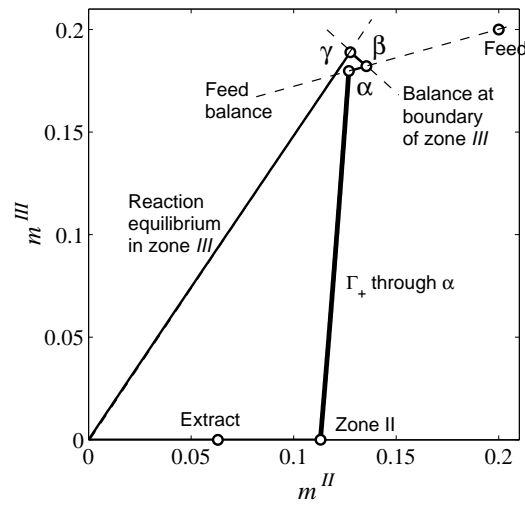


**Figure 5.2** – Illustration for the example of producing the stronger adsorbing enantiomer by process 5 in Fig. 2 [PII-10] with a heterogeneous reaction in zone III. Symbols – prediction from equilibrium theory, dashed – balances mentioned in the text, solid – TMB model. Parameters: 400 stages per zone,  $k_{het} = 10^6$ .  $m_{I...III} = (25.0, 13.6, 15.395)$ , bi-Langmuir isotherms from [PII-10].

This is illustrated for the production of a stronger adsorbing enantiomer by process 5 in Fig. 2 [PII-10] with a heterogeneous reaction taking place in zone III. The states  $\alpha$  and  $\beta$  are those left and right of the feed  $F$ . For stream  $\beta$ , which “hits” the reactive boundary, holds  $C = c_{A,\beta} + c_{B,\beta}$ . This is subjected to reaction equilibrium according to

$$c_A^* = C \frac{K'_{eq}}{1 + K'_{eq}}, \quad (5.13a)$$

$$c_B^* = C \frac{1}{1 + K'_{eq}}. \quad (5.13b)$$

State  $\gamma$  is the composition of the solid leaving the reactive boundary and entering zone II, which is in adsorption equilibrium with the  $c_i^*$  above. The composition in zone II is found from the slope of the  $\Gamma_+$  characteristic through  $\alpha$  as explained in the shortcut method in Section 3.3.1 and shown in the figure. The composition of the extract  $E$  follows from a simple mass balance around the process.

In a similar manner the design problem can be solved for the remaining three configurations. This is shown in Fig. 5.3. The good agreement with numerically determined separation regions confirms that the developed shortcut design method is suitable for the integrated 3-zone processes.

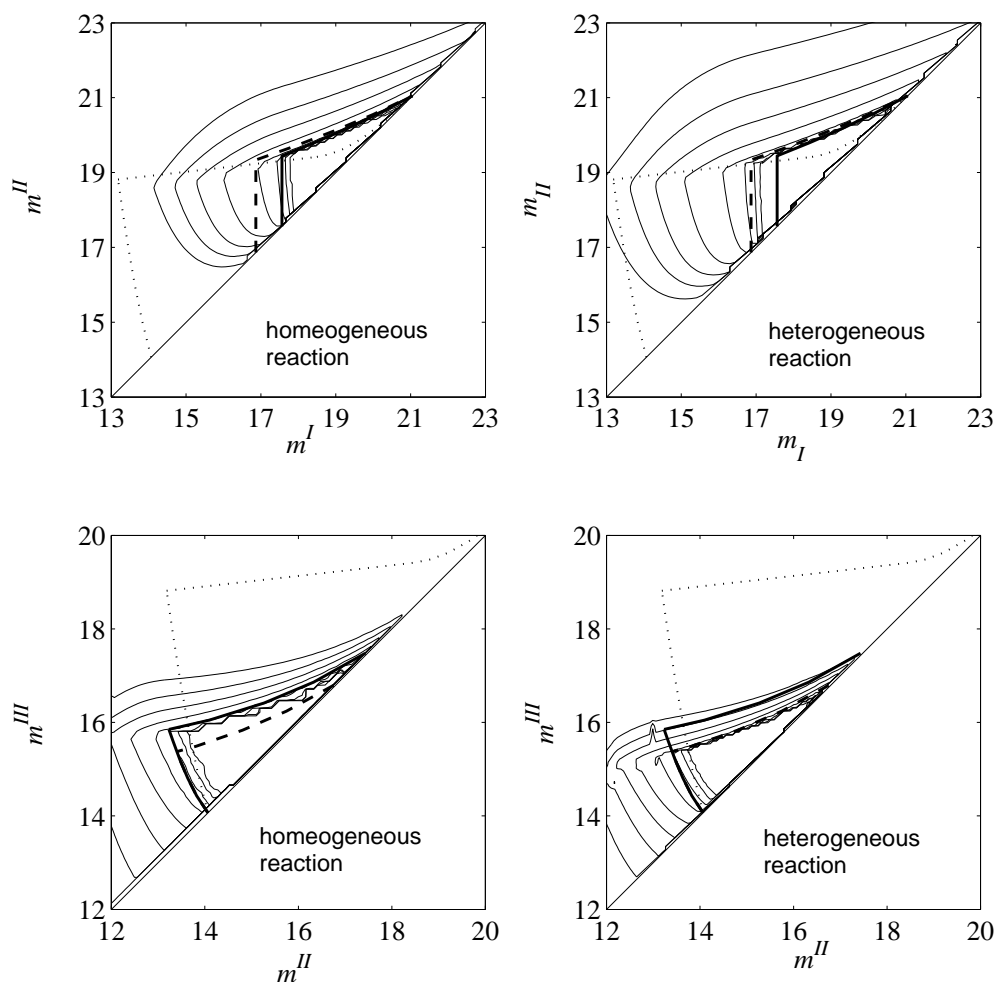


**Figure 5.3** – Regions of complete separation predicted for the four possible process configurations of the 3-zone process. Top – production of the weaker adsorbed component  $B$ , cf. Fig. 1 [PII-10]. Bottom – stronger adsorbing component  $A$ , cf. Fig. 2 [PII-10]. Homogeneous reaction (solid, thick lines) vs. heterogeneous reaction (dashed, thick). Numerically determined regions (solid, thin) shown for purities of 80, 90, 95, 99, 99.9, 99.99, 99.999 and 100 %, respectively. Also for comparison is shown the separation region for a non-reactive four-zone process (dotted) as determined by the method in Section 3.3.1.

Parameters: TMB model with 400 stages per zone, feed  $c_{F,i} = 0.2$  g/L,  $K_{eq} = K'_{eq} = 1$ , reaction rate constants  $10^5$  min $^{-1}$ . bi-Langmuir isotherms in [PII-10].

### 5.2.4 Experimental Validation of a Developed 3-zone Process

In the previous sections an integrated 3-zone SMB process was developed that was projected to be capable of producing a single pure enantiomer from a racemic mixture, thereby increasing the yield of such production from 50 to 100%. Below a summary of its experimental validation is given as published in [PII-11].

The enantiomers of Chlorthalidone (CTD) served again as model system. CTD is known to racemize spontaneously at ambient conditions, with a reaction rate depending significantly on temperature and pH value [168, 169]. This lets one expect that a sufficient ratio of the reaction rate, see Section 5.2.2, can be adjusted within the process by either a temperature or pH gradient, respectively. As demonstrated in [PII-9] the pH allows for the stronger manipulation.

In a first step, the initial data on the racemization kinetics as function of temperature in [152] are extended by determining them also as function of the pH value in the range pH=5.3...9.0. Compared to the acidic conditions (pH = 1.0...6.5) applied by Lamparter [169] the reaction rate increases drastically towards pH = 9.0, see Fig. 4 [PII-11].

Regarding the desired strong change of the reactivity within the SMB process, a step gradient from pH=5.3 to 9.0 corresponds to a ratio of the rate constants of 5600, which is much higher than attainable by a temperature shift (*cf.* [152]).

Accordingly, the adsorption isotherms of the CTD enantiomers were determined in this pH range by the inverse method. A bi-Langmuir model with the saturation capacity of the achiral site expressed as a sigmoidal function of the pH value gives a sufficient model accuracy, see Fig. 6 [PII-11].

The determined parameters are used in an SMB model to design the process. Goal is to produce the weaker adsorbing enantiomer at a purity of 100%. It is worth mentioning that this can hardly be accomplished by a Hashimoto setup [170].

Scanning the corresponding region of  $m$ -values yields the operating region shown in Fig. 7 [PII-11]. This suggests that a sufficiently large parameter range exists where a pure enantiomer can be produced.

The concept is then investigated experimentally at bench scale for several operating points. The 2-zone open-loop system in Fig. 2 [PII-11] was equipped with two 6.5 x 1.6cm columns per zone. The chosen setup facilitates monitoring the functioning of the reaction assisted regeneration in zone  $I$  in an additional zone shown on the right in Fig. 2 [PII-11]. The additional zone in the middle was used only to have a symmetrical setup within the used 16-port carousel SMB system.

The purities achieved in the experiments correspond to the design predictions as summarized in Tab. 3 <sup>[PII-11]</sup>. Values up to the detection limit of 98% were achieved and the occurrence of a reaction-assisted regeneration was affirmed. Small amounts of side products could be reduced by adjusting the feed strategy.

The obtained results confirm that this integrated process is capable of producing a pure single enantiomer at a yield of 100%. The concept can be extended to other types of “reactive” gradients, for example, gradients of temperature, modifiers or additives, homogeneous catalysts, enzymes, or inhibitors of heterogeneous catalysts. It should be readily applicable to further enantiomeric systems and other isomerization problems, provided the compound of interest allows for a sufficient tuning of the reaction rate by a suitable gradient.

## Concluding Remarks

The processes and design methods discussed in this work were devised with the goal of further improving the performance and applicability of chromatography for challenging industrial separation problems.

The concepts elucidated in the frame of advanced operating modes demonstrate that a significant potential exists for enhancing the performance of chromatographic separations. The theoretical and experimental results obtained for SSR chromatography underline that such achievements can be made even on the basis of simple process setups. The shortcut design methods for SSR and SMB processes that were developed on the basis of equilibrium theory could help lowering the hurdles for practitioners who are interested in applying these technologies.

Combining chromatography with other separation processes or (bio)chemical reactions exhibits several options to enhance performance. The developed design methods for SMB and SSR chromatography for limited purity requirements are particularly useful for this type of processes. Promising results were obtained in first steps towards industrial implementation of a sophisticated combined process. The optimization-based synthesis of flowsheets was found a viable strategy to cope with the multitude of process alternatives.

Although the considered concepts are based on rather simple ideas, they pose challenges that deserve further practical and theoretical studies related to, for example, their implementation as fully continuous schemes and the dynamic behavior and control of such combined processes.

Finally, also reactive chromatography offers interesting prospects. A new process concept was developed that is suitable for the challenging problem of producing of a pure enantiomer from a racemate at complete yield. Using a generic approach, first the optimal properties of the process were identified and analyzed, before it was translated into a process setup and finally also validated successfully. It is expected that the concept can be extended in different directions and utilized in further application areas.



## References

- [1] G. Guiochon, D. G. Shirazi, A. Felinger, and A. M. Katti. *Fundamentals of Preparative and Nonlinear Chromatography*. 2nd Edition, Academic Press, Boston, USA, 2006.
- [2] K. Sundmacher, A. Kienle, and A. Seidel-Morgenstern (Eds.). *Integrated Chemical Processes*. Wiley-VCH, 2005.
- [3] A. Tiselius. Displacement development in adsorption analysis. *Arkiv Kemi Min Geol A* 16A (1943) 1–11.
- [4] R. S. Alm, R. J. P. Williams, and A. Tiselius. Gradient Elution Analysis – I. A General Treatment. *Acta Chem Scand* 6 (1952) 826–836.
- [5] K. Anton and C. Berger (Eds.). *Supercritical Fluid Chromatography with Packed Columns: Techniques and applications*. Marcel Dekker, 1998.
- [6] B. Sreedhar and A. Seidel-Morgenstern. Preparative separation of multi-component mixtures using stationary phase gradients. *J Chromatogr A* 1215 (2008) 133 – 144.
- [7] P. Jandera and J. Churáček. *Gradient Elution in Column Liquid Chromatography: Theory and Practice*. Elsevier Science, Amsterdam, 1985.
- [8] L. R. Snyder and J. W. Dolan. *High-Performance Gradient Elution: The Practical Application of the Linear-Solvent-Strength Model*. John Wiley & Sons, Hoboken, New Jersey, 2007.
- [9] K. Bombaugh, W. Dark, and R. Levangie. High resolution steric chromatography. *J Chromatogr Sci* 7 (1969) 42.
- [10] A. Seidel-Morgenstern and G. Guiochon. Theoretical Study of Recycling in Preparative Chromatography. *AIChE J* 39 (1993) 809–819.
- [11] C. Heuer, A. Seidel-Morgenstern, and P. Hugo. Experimental investigation and modelling of closed-loop recycling in preparative chromatography. *Chem Eng Sci* 50 (1995) 1115–1127.
- [12] M. Bailly and D. Tondeur. Recycle optimization in non-linear productive chromatography – I Mixing recycle with fresh feed. *Chem Eng Sci* 37 (1982) 1199–1212.
- [13] C. M. Grill. Closed-loop recycling with periodic intra-profile injection: a new binary preparative chromatographic technique. *J Chromatogr A* 796 (1998) 101–113.
- [14] G. Ziomek, D. Antos, L. Tobiska, and A. Seidel-Morgenstern. Comparison of possible arrangements of five identical columns in preparative chromatography. *J Chromatogr A* 1116 (2006) 179–188.

- [15] M. Sardin and J. Villiermaux. Synthese de l'Acetate de Mentyle par Chromatographie Reactive. *Chem Eng J* 30 (1985) 91–101.
- [16] M. Sardin, D. Schweich, and J. Villiermaux. In: G. Ganetsos and P. Barker (Eds.): Preparative and Production Scale Chromatography., vol. 61. Chapter: Preparative fixed-bed chromatographic reactor. Marcel Dekker, 1993 477–521.
- [17] M. Mazzotti, D. Gelosa, B. Neri, and M. Morbidelli. Dynamics of a chromatographic reactor: esterification catalysed by acidic resins. *Ind Eng Chem Res* 36 (1997) 3163–3172.
- [18] D. Gelosa, M. Ramaioli, G. Valente, and M. Morbidelli. Chromatographic Reactors: Esterification of Glycerol with Acetic Acid Using Acidic Polymeric Resins. *Ind Eng Chem Res* 42 (2003) 6536–6544.
- [19] D. Gelosa, A. Sliepcevich, and M. Morbidelli. Chromatographic Reactors with Reactive Desorbents. *Ind Eng Chem Res* 45 (2006) 3922–3925.
- [20] T. Falk and A. Seidel-Morgenstern. Comparison between a fixed-bed reactor and a chromatographic reactor. *Chem Eng Sci* 54 (1999) 1479–1485.
- [21] P. T. Mai, T. D. Vu, K. X. Mai, and A. Seidel-Morgenstern. Analysis of Heterogeneously Catalyzed Ester Hydrolysis Performed in a Chromatographic Reactor and in a Reaction Calorimeter. *Ind Eng Chem Res* 43 (2004) 4691–4702.
- [22] T. D. Vu, A. Seidel-Morgenstern, S. Grüner, and A. Kienle. Analysis of Ester Hydrolysis Reactions in a Chromatographic Reactor using Equilibrium Theory and a Rate Model. *Ind Eng Chem Res* 44 (2005) 9565–9574.
- [23] G. Ströhlein, Y. Assuncao, N. Dube, A. Bardow, M. Mazzotti, and M. Morbidelli. Esterification of acrylic acid with methanol by reactive chromatography: Experiments and simulations. *Chem Eng Sci* 61 (2006) 5296–5306.
- [24] C. B. Ching and D. M. Ruthven. Experimental-study of a simulated countercurrent adsorption system – IV. Non-isothermal operation. *Chem Eng Sci* 41 (1986) 3063–3071.
- [25] C. Migliorini, M. Wendlinger, M. Mazzotti, and M. Morbidelli. Temperature gradient operation of a simulated moving bed unit. *Ind Eng Chem Res* 40 (2001) 2606–2617.
- [26] J. Kim, N. Abunasser, P. Wankat, A. Stawarz, and Y.-M. Koo. Thermally Assisted Simulated Moving Bed Systems. *Adsorption* 11 (2005) 579–584.
- [27] W. Jin and P. C. Wankat. Thermal operation of four-zone simulated moving beds. *Ind Eng Chem Res* 46 (2007) 7208–7220.
- [28] T. B. Jensen, T. G. Reijns, H. A. Billiet, and L. A. van der Wielen. Novel simulated moving-bed method for reduced solvent consumption. *J Chromatogr A* 873 (2000) 149–162.
- [29] D. Antos and A. Seidel-Morgenstern. Application of gradients in simulated moving

- bed processes. *Chem Eng Sci* 56 (2001) 6667–6682.
- [30] S. Abel, M. Mazzotti, and M. Morbidelli. Solvent gradient operation of simulated moving beds. I. Linear isotherms. *J Chromatogr A* 944 (2002) 23–39.
- [31] S. Abel, M. Mazzotti, and M. Morbidelli. Solvent gradient operation of simulated moving beds. II. Langmuir isotherms. *J Chromatogr A* 1026 (2004) 47–55.
- [32] S. Abel. Design and Operation of Simulated Moving Bed Processes for Fine Chemical and Pharmaceutical Separations. Ph.D. thesis, Eidgenössische Technische Hochschule Zürich (2004).
- [33] N. Gottschlich and V. Kasche. Purification of monoclonal antibodies by simulated moving-bed chromatography. *J Chromatogr A* 765 (1997) 201–206.
- [34] J. Houwing, S. H. van Hateren, H. A. H. Billiet, and L. A. M. van der Wielen. Effect of salt gradients on the separation of dilute mixtures of proteins by ion-exchange in simulated moving beds. *J Chromatogr A* 952 (2002) 85–98.
- [35] J. Houwing, T. B. Jensen, S. H. van Hateren, H. A. H. Billiet, and L. A. M. van der Wielen. Positioning of salt gradients in ion-exchange SMB. *AIChE J* 49 (2003) 665–674.
- [36] L. Gueorguieva, L. F. Vallejo, U. Rinas, and A. Seidel-Morgenstern. Discontinuous and continuous separation of the monomeric and dimeric forms of human bone morphogenetic protein-2 from renaturation batches. *J Chromatogr A* 1135 (2006) 142–150.
- [37] P. Li, G. H. Xiu, and A. E. Rodrigues. Proteins separation and purification by salt gradient ion-exchange SMB. *AIChE J* 53 (2007) 2419–2431.
- [38] R.-M. Nicoud, M. Perrut, and G. Hotier. Method and apparatus for fractionation of a mixture on a simulated fluidized bed in the presence of a compressed gas, a supercritical fluid or a subcritical liquid. U.S. patent 5 422 007 (1995).
- [39] J.-Y. Clavier, R. M. Nicoud, and M. Perrut. In: P. R. von Rohr and C. Trepp (Eds.): High-Pressure Chemical Engineering. Chapter: A new efficient fractionation process: The simulated moving bed with supercritical eluent. Elsevier Science, London, 1996.
- [40] M. Mazzotti, G. Storti, and M. Morbidelli. Supercritical fluid simulated moving bed chromatography. *J Chromatogr A* 786 (1997) 309–320.
- [41] O. D. Giovanni, M. Mazzotti, M. Morbidelli, F. Denet, W. Hauck, and R. M. Nicoud. Supercritical fluid simulated moving bed chromatography II. Langmuir isotherm. *J Chromatogr A* 919 (2001) 1–12.
- [42] A. Depta, T. Giese, M. Johannsen, and G. Brunner. Separation of stereoisomers in a simulated moving bed-supercritical fluid chromatography plant. *J Chromatogr A* 865 (1999) 175–186.
- [43] M. Johannsen, S. Peper, and A. Depta. Simulated moving bed chromatography

- with supercritical fluids for the resolution of bi-naphthol enantiomers and phytol isomers. *J Biochem Bioph Meth* 54 (2002) 85–102.
- [44] S. Abdelmoumen, L. Muhr, M. Bailly, and O. Ludemann-Hombourger. The M3C Process: A New Multicolumn Chromatographic Process Integrating a Concentration Step. I - The Equilibrium Model. *Sep Sci Technol* 41 (2006) 2639–2663.
- [45] G. Paredes, H. K. Rhee, and M. Mazzotti. Design of simulated-moving-bed chromatography with enriched extract operation (EE-SMB): Langmuir isotherms. *Ind Eng Chem Res* 45 (2006) 6289–6301.
- [46] J. S. Hur and P. C. Wankat. Hybrid simulated moving bed and chromatography systems for center-cut separation from quaternary mixtures: Linear isotherm systems. *Ind Eng Chem Res* 45 (2006) 8713–8722.
- [47] L. C. Keßler and A. Seidel-Morgenstern. Theoretical study of multicomponent continuous countercurrent chromatography based on connected 4-zone units. *J Chromatogr A* 1126 (2006) 323–337.
- [48] R. Wooley, Z. Ma, and N. H. L. Wang. A nine-zone simulating moving bed for the recovery of glucose and xylose from biomass hydrolyzate. *Ind Eng Chem Res* 37 (1998) 3699–3709.
- [49] Y. A. Beste and W. Arlt. Side-Stream Simulated Moving-Bed Chromatography for Multicomponent Separation. *Chem Eng Technol* 25 (2002) 956–962.
- [50] J. K. Kim, Y. F. Zang, and P. C. Wankat. Single-cascade simulated moving bed systems for the separation of ternary mixtures. *Ind Eng Chem Res* 42 (2003) 4849–4860.
- [51] J. S. Hur and P. C. Wankat. New design of simulated moving bed (SMB) for ternary separations. *Ind Eng Chem Res* 44 (2005) 1906–1913.
- [52] S. Abel, M. U. Bäßler, C. Arpagaus, M. Mazzotti, and J. Stadler. Two-fraction and three-fraction continuous simulated moving bed separation of nucleosides. *J Chromatogr A* 1043 (2004) 201–210.
- [53] G. Paredes, S. Abel, M. Mazzotti, M. Morbidelli, and J. Stadler. Analysis of a Simulated Moving Bed Operation for Three-Fraction Separations (3F-SMB). *Ind Eng Chem Res* 43 (2004) 6157–6167.
- [54] M. Kearney and K. Hieb. Time variable simulated moving bed process. US patent 5 102 553 (1992).
- [55] E. Kloppenburg and E. D. Gilles. A new concept for operating simulated moving-bed processes. *Chem Eng Technol* 22 (1999) 813–817.
- [56] Z. Zhang, M. Mazzotti, and M. Morbidelli. PowerFeed operation of simulated moving bed units: changing flow-rates during the switching interval. *J Chromatogr A* 1006 (2003) 87–99.
- [57] O. Ludemann-Hombourger, R. Nicoud, and M. Bailly. The “VariCol” process: a

- new multicolumn continuous chromatographic process. *Sep Sci Technol* 35 (2000) 1829–1862.
- [58] Z. Zhang, K. Hidajat, A. K. Ray, and M. Morbidelli. Multiobjective Optimization of SMB and Varicol Process for Chiral Separation. *AIChE J* 48 (2002) 2800–2816.
- [59] H. Schramm, M. Kaspereit, A. Kienle, and A. Seidel-Morgenstern. Improving Simulated Moving Bed Processes by Cyclic Modulation of the Feed Concentration. *Chem Eng Technol* 25 (2002) 1151–1155.
- [60] H. Schramm, A. Kienle, M. Kaspereit, and A. Seidel-Morgenstern. Improved operation of simulated moving bed processes through cyclic modulation of feed flow and feed concentration. *Chem Eng Sci* 58 (2003) 5217–5227.
- [61] H. Schramm, M. Kaspereit, A. Kienle, and A. Seidel-Morgenstern. Simulated moving bed process with cyclic modulation of the feed concentration. *J Chromatogr A* 1006 (2003) 77–86.
- [62] Z. Zhang, M. Mazzotti, and M. Morbidelli. Continuous Chromatographic Processes with a Small Number of Columns: Comparison of Simulated Moving Bed with Varicol, PowerFeed, and ModiCon. *Korean J Chem Eng* 21 (2004) 454–464.
- [63] Y. Kawajiri and L. T. Biegler. Large scale nonlinear optimization for asymmetric operation and design of Simulated Moving Beds. *J Chromatogr A* 1133 (2006) 226–240.
- [64] Y. Zang and P. C. Wankat. SMB Operation Strategy – Partial Feed. *Ind Eng Chem Res* 41 (2002) 2504–2511.
- [65] Y. Zang and P. C. Wankat. Three-Zone Simulated Moving Bed with Partial Feed and Selective Withdrawal. *Ind Eng Chem Res* 41 (2002) 5283–5289.
- [66] D. Acetti, C. Langel, E. Brenna, C. Fuganti, and M. Mazzotti. Intermittent simulated moving bed chromatographic separation of (RS,RS)-2-(2,4-difluorophenyl)butane-1,2,3-triol. *J Chromatogr A* 1217 (2010) 2840 – 2846.
- [67] S. Katsuo and M. Mazzotti. Intermittent simulated moving bed chromatography: 1. Design criteria and cyclic steady-state. *J Chromatogr A* 1217 (2010) 1354–1361.
- [68] S. Katsuo and M. Mazzotti. Intermittent simulated moving bed chromatography: 2. Separation of Tröger’s base enantiomers. *J Chromatogr A* 1217 (2010) 3067 – 3075.
- [69] Y.-S. Bae and C.-H. Lee. Partial-discard strategy for obtaining high purity products using simulated moving bed chromatography. *J Chromatogr A* 1122 (2006) 161–173.
- [70] L. C. Keßler and A. Seidel-Morgenstern. Improving performance of simulated moving bed chromatography by fractionation and feed-back of outlet streams. *J Chromatogr A* 1207 (2008) 55 – 71.
- [71] S. Li, Y. Kawajiri, J. Raisch, and A. Seidel-Morgenstern. Optimization of simulated

- moving bed chromatography with fractionation and feedback: Part I. Fractionation of one outlet. *J Chromatogr A* 1217 (2010) 5337 – 5348.
- [72] S. Li, Y. Kawajiri, J. Raisch, and A. Seidel-Morgenstern. Optimization of simulated moving bed chromatography with fractionation and feedback: Part II. Fractionation of both outlets. *J Chromatogr A* 1217 (2010) 5349 – 5357.
- [73] G. Ströhlein, L. Aumann, M. Mazzotti, and M. Morbidelli. A continuous, counter-current multi-column chromatographic process incorporating modifier gradients for ternary separations. *J Chromatogr A* 1126 (2006) 338–346.
- [74] J. S. Hur and P. C. Wankat. Two-zone SMB/chromatography for center-cut separation from ternary mixtures: Linear isotherm systems. *Ind Eng Chem Res* 45 (2006) 1426–1433.
- [75] K. Hashimoto, S. Adachi, H. Noujima, and Y. Ueda. A new process combining adsorption and enzyme reaction for producing higher-fructose syrup. *Biotechnol Bioeng* 25 (1983) 2371–2393.
- [76] B. Cho, R. Aris, and R. Carr. The mathematical theory of a countercurrent catalytic reactor. *Proc R Soc Lond A* 383 (1982) 147–189.
- [77] A. K. Ray, R. W. Carr, and R. Aris. The Simulated Countercurrent Moving Bed Chromatographic Reactor – A Novel Reactor-Separator. *Chem Eng Sci* 49 (1994) 469–480.
- [78] A. Y. Tonkovich and R. W. Carr. Modeling of the Simulated Countercurrent Moving-Bed Chromatographic Reactor used for the Oxidative Coupling of Methane. *Chem Eng Sci* 49 (1994) 4657–4665.
- [79] A. Y. Tonkovich and R. W. Carr. A Simulated Countercurrent Moving-Bed Chromatographic Reactor for the Oxidative Coupling of Methane: Experimental Results. *Chem Eng Sci* 49 (1994) 4647–4656.
- [80] A. K. Ray and R. W. Carr. Experimental Study of a Laboratory-scale Simulated Countercurrent Moving Bed Chromatographic Reactor. *Chem Eng Sci* 50 (1995) 2195–2202.
- [81] A. V. Kruglov, M. C. Bjorklund, and R. W. Carr. Optimization of the Simulated Countercurrent Moving-Bed Chromatographic Reactor for the oxidative Coupling of Methane. *Chem Eng Sci* 51 (1996) 2945–2950.
- [82] M. Mazzotti, A. Kruglov, B. Neri, D. Gelosa, and M. Morbidelli. A Continuous Chromatographic Reactor: SMBR. *Chem Eng Sci* 51 (1996) 1827–1836.
- [83] F. Lode, M. Houmard, C. Migliorini, M. Mazzotti, and M. Morbidelli. Continuous reactive chromatography. *Chem Eng Sci* 56 (2001) 269–291.
- [84] H.-K. Rhee, R. Aris, and N. R. Amundson. First-order Partial Differential Equations. Vol. II - Theory and Applications of Hyperbolic Systems of Quasilinear Equations. Dover Publications, 2001.

- [85] S. Grüner and A. Kienle. Equilibrium theory and nonlinear waves for reactive distillation columns and chromatographic reactors. *Chem Eng Sci* 59 (2004) 901–918.
- [86] S. Grüner, M. Mangold, and A. Kienle. Dynamics of reaction separation processes in the limit of chemical equilibrium. *AIChE J* 52 (2006) 1010–1026.
- [87] J. Blehaut and R.-M. Nicoud. Recent aspects in simulated moving bed. *Analysis Mag* 26 (1998) M60–M70.
- [88] P. S. Gomes, M. Minceva, and A. E. Rodrigues. Simulated moving bed technology: old and new. *Adsorption* 12 (2006) 375–392.
- [89] A. Seidel-Morgenstern, L. C. Keßler, and M. Kaspereit. New Developments in Simulated Moving Bed Chromatography. *Chem Eng Technol* 31 (2008) 826–837.
- [90] A. Seidel-Morgenstern, L. C. Keßler, and M. Kaspereit. Neue Entwicklungen auf dem Gebiet der simulierten Gegenstromchromatographie. *Chem Ing Tech* 80 (2008) 725–740.
- [91] H. Schmidt-Traub (Ed.). Preparative chromatography of fine chemical and pharmaceutical agents. Wiley-VCH, Weinheim, 2005.
- [92] D. B. Broughton and C. G. Gerhold;. Continuous Sorption Process Employing Fixed Bed of Sorbent and Moving Inlets and Outlets. U.S. Patent 2 985 589 (1961).
- [93] C. Y. Chin and N.-H. L. Wang. Simulated Moving Bed Equipment Designs. *Sep Purif Rev* 33 (2004) 77–155.
- [94] M. Czok and G. Guiochon. The physical sense of simulation models of liquid chromatography: propagation through a grid or solution of the mass balance equation. *Anal Chem* 62 (1990) 189–200.
- [95] G. Guiochon and B. Lin. Modeling for Preparative Chromatography. Academic Press, San Diego, USA, 2003.
- [96] A. Seidel-Morgenstern. Mathematische Modellierung der präparativen Flüssigchromatographie. Deutscher Universitätsverlag, Wiesbaden, 1995.
- [97] D. Antos. Gradient techniques in preparative chromatography – Modelling and experimental realization. Oficyna Wydawnicza Politechniki Rzeszowskiej, Rzeszów, Poland, 2003.
- [98] P. Rouchon, M. Schonauer, P. Valentin, and G. Guiochon. Numerical Solution of Band Propagation in Nonlinear Chromatography. *Sep Sci Technol* 22 (1987) 1793–1833.
- [99] A. J. P. Martin and R. L. M. Synge. A new form of chromatogram employing two liquid phases. *Biochem J* 35 (1941) 1358–1368.
- [100] L. C. Craig. Identification of Small Amounts of Organic Compounds by Distribution Studies. II. Separation By Counter-current Distribution. *J Biol Chem* 155 (1944) 519–534.

- [101] J. Wilson. A theory of chromatography. *J Am Chem Soc* 62 (1940) 1583–1591.
- [102] J. Weiss. 81. On the theory of chromatography. *J Chem Soc* (1943) 297–303.
- [103] D. DeVault. The Theory of Chromatography. *J Am Chem Soc* 65 (1943) 532–540.
- [104] E. Glückauf. Contributions to the theory of chromatography. *P Roy Soc Lond A Mat* 186 (1946) 35–57.
- [105] E. Glückauf. Theory of chromatography. Part II. Chromatograms of a single solute. *J Chem Soc* (1947) 1302–1308.
- [106] E. Glückauf. Theory of chromatography. VII. The general theory of two solutes following non-linear isotherms. *Discuss Faraday Soc* 7 (1949) 12–25.
- [107] P. D. Lax. Hyperbolic systems of conservation laws II. *Comm Pure Appl Math* 10 (1957) 537–566.
- [108] F. G. Helfferich. Multicomponent Ion Exchange in Fixed Beds. Generalized Equilibrium Theory for Systems with Constant Separation Factors. *Ind Eng Chem Fund* 6 (1967) 362–364.
- [109] F. Helfferich and G. Klein. Multicomponent chromatography. Marcel Dekker, New York, 1970.
- [110] H.-K. Rhee, R. Aris, and N. R. Amundson. On the Theory of Multicomponent Chromatography. *Philos T Roy Soc A* 267 (1970) 419–455.
- [111] G. Guiochon and S. Golshan-Shirazi. A retrospective on the solution of the ideal model of chromatography. *J Chromatogr A* 658 (1994) 173 – 177.
- [112] H.-K. Rhee, R. Aris, and N. R. Amundson. First-order Partial Differential Equations. Vol. I – Theory and Applications of Single Equations. Dover Publications, 2001.
- [113] G. Storti, M. Mazzotti, M. Morbidelli, and S. Carrà. Robust design of binary countercurrent adsorption separation processes. *AIChE J* 39 (1993) 471–492.
- [114] M. Mazzotti, G. Storti, and M. Morbidelli. Robust design of countercurrent adsorption separation processes: 2. Multicomponent systems. *AIChE J* 40 (1994) 1825–1842.
- [115] M. Mazzotti, G. Storti, and M. Morbidelli. Robust design of countercurrent adsorption separation: 3. Nonstoichiometric systems. *AIChE J* 42 (1996) 2784–2796.
- [116] M. Mazzotti, G. Storti, and M. Morbidelli. Robust design of countercurrent adsorption separation processes: 4. Desorbent in the feed. *AIChE J* 43 (1997) 64–72.
- [117] C. Migliorini, M. Mazzotti, and M. Morbidelli. Robust design of countercurrent adsorption separation processes: 5. Nonconstant selectivity. *AIChE J* 46 (2000) 1384–1399.
- [118] A. Seidel-Morgenstern. Experimental determination of single solute and competitive adsorption isotherms. *J Chromatogr A* 1037 (2004) 255–272.

- [119] I. Langmuir. The Constitution And Fundamental Properties Of Solids And Liquids. Part I. Solids. *J Am Chem Soc* 38 (1916) 2221–2295.
- [120] D. Graham. The Characterization of Physical Adsorption Systems. I. The Equilibrium Function and Standard Free Energy of Adsorption. *J Phys Chem* 57 (1953) 665–669.
- [121] S. Jacobson, S. Golshan-Shirazi, and G. Guiochon. Isotherm selection for band profile simulations in preparative chromatography. *AIChE J* 37 (1991) 836–844.
- [122] A. Kienle. Nichtlineare Wellenphänomene und Stabilität stationärer Zustände in Destillationskolonnen. Fortschrittsberichte Reihe 3 Nr. 506, VDI Verlag, Düsseldorf, 1997.
- [123] E. Kvaalen, L. Neel, and D. Tondeur. Directions of quasi-static mass and energy transfer between phases in multicomponent open systems: Implications in separation science. *Chem Eng Sci* 40 (1985) 1191 – 1204.
- [124] D. Flockerzi, M. Kaspereit, and A. Kienle. Spectral properties of modified Langmuir and Bi-Langmuir isotherms. *Chem Eng Sci* (subm.).
- [125] F. G. Helfferich and P. W. Carr. Non-linear waves in chromatography : I. Waves, shocks, and shapes. *J Chromatogr A* 629 (1993) 97–122.
- [126] M. Mazzotti. Equilibrium theory based design of simulated moving bed processes for a generalized Langmuir isotherm. *J Chromatogr A* 1126 (2006) 311–322.
- [127] M. Mazzotti. Design of Simulated Moving Bed Separations: Generalized Langmuir Isotherm. *Ind Eng Chem Res* 45 (2006) 6311–6324.
- [128] M. Mazzotti, G. Storti, and M. Morbidelli. Optimal operation of simulated moving bed units for nonlinear chromatographic separations. *J Chromatogr A* 769 (1997) 3–24.
- [129] M. F. Doherty and G. Buzad. Reactive distillation by design. *TI Chem Eng-Lond* 70 (1992) 448–458.
- [130] H.-K. Rhee and N. R. Amundson. An Analysis of an Adiabatic Adsorption Column: Part I. Theoretical Development. *Chem Eng J* 1 (1970) 241–254.
- [131] T. Fornstedt and G. Guiochon. Theoretical Study of High-Concentration Elution Profiles and Large System Peaks in Nonlinear Chromatography. *Anal Chem* 66 (1994) 2116–2128.
- [132] T. Fornstedt and G. A. Guiochon. Comparison between Experimental and Theoretical Profiles of High Concentration Elution Bands and Large System Peaks in Nonlinear Chromatography. *Anal Chem* 66 (1994) 2686–2693.
- [133] R. Arnell, P. Forssen, and T. Fornstedt. Tuneable peak deformations in chiral liquid chromatography. *Anal Chem* 79 (2007) 5838–5847.
- [134] G. Ströhlein, M. Mazzotti, and M. Morbidelli. Analysis of sample-solvent induced modifier-solute peak interactions in biochromatography using equilibrium theory

- and detailed simulations. *J Chromatogr A* 1091 (2005) 60–71.
- [135] G. Ströhlein, L. Aumann, L. Melter, K. Buscher, B. Schenkel, M. Mazzotti, and M. Morbidelli. Experimental verification of sample-solvent induced modifier-solute peak interactions in biochromatography. *J Chromatogr A* 1117 (2006) 146–153.
- [136] I. Duvdevani, J. A. Biesenberger, and M. Tan. Recycle gel permeation chromatography. III. Design modifications and some results with polycarbonate. *J Polym Sci B* 9 (1971) 429–434.
- [137] M. Kaspereit, K. Geddicke, A. W. Zahn, V. Mahoney, and A. Seidel-Morgenstern. Shortcut method for evaluation and design of a hybrid process for enantioseparations. *J Chromatogr A* 1092 (2005) 43–54.
- [138] D. Schlinge, P. Scherpian, and G. Schembecker. Comparison of process concepts for preparative chromatography. *Chem Eng Sci* 65 (2010) 5373–5381.
- [139] P. Scherpian and G. Schembecker. Scaling-up recycling chromatography. *Chem Eng Sci* 64 (2009) 4068 – 4080.
- [140] F. Charton, M. Bailly, and G. Guiochon. Recycling in preparative liquid chromatography. *J Chromatogr A* 687 (1994) 13–31.
- [141] I. Quiñones, C. Grill, L. Miller, and G. Guiochon. Modeling of separations by closed-loop steady-state recycling chromatography of a racemic pharmaceutical intermediate. *J Chromatogr A* 867 (2000) 1–21.
- [142] G. Storti, R. Baciocchi, M. Mazzotti, and M. Morbidelli. Design of Optimal Operating Conditions of Simulated Moving Bed Adsorptive Separation Units. *Ind Eng Chem Res* 34 (1995) 288–301.
- [143] A. Rajendran. Equilibrium theory-based design of simulated moving bed processes under reduced purity requirements: Linear isotherms. *J Chromatogr A* 1185 (2008) 216 – 222.
- [144] B.-G. Lim, C.-B. Ching, R. B. H. Tan, and S.-C. Ng. Recovery of (–)-praziquantel from racemic mixtures by continuous chromatography and crystallisation. *Chem Eng Sci* 50 (1995) 2289–2298.
- [145] H. Lorenz, P. Sheehan, and A. Seidel-Morgenstern. Coupling of simulated moving bed chromatography and fractional crystallisation for efficient enantioseparation. *J Chromatogr A* 908 (2001) 201–14.
- [146] M. Kaspereit. Separation of Enantiomers by a Process Combination of Chromatography and Crystallisation. Shaker Verlag, Aachen, Germany, 2006.
- [147] M. Amanullah and M. Mazzotti. Optimization of a hybrid chromatography-crystallization process for the separation of Tröger's base enantiomers. *J Chromatogr A* 1107 (2006) 36–45.
- [148] K. Geddicke, M. Kaspereit, W. Beckmann, U. Budde, H. Lorenz, and A. Seidel-

- Morgenstern. Conceptual Design & Feasibility Study of Combining Continuous Chromatography and Crystallisation for Stereoisomer Separations. *Chem Eng Res Des* 85 (2007) 928–936.
- [149] T. Borren and H. Schmidt-Traub. Vergleich chromatographischer Reaktorkonzepte. *Chem Ing Tech* 76 (2004) 805–814.
- [150] M. Bechtold, S. Makart, M. Heinemann, and S. Panke. Integrated operation of continuous chromatography and biotransformations for the generic high yield production of fine chemicals. *J Biotechnol* 124 (2006) 146 – 162.
- [151] T. Borren. Untersuchungen zu chromatographischen Reaktoren mit verteilten Funktionalitäten. Fortschritt-Berichte VDI : Reihe 3, Verfahrenstechnik 876, 2007.
- [152] M. Kaspereit, J. García Palacios, T. Meixús Fernández, and A. Kienle. In: B. Braunschweig and X. Joulia (Eds.): *Computer-Aided Chemical Engineering*, vol. 25 – 18<sup>th</sup> Europ. Symp. Comp. Aid. Proc. Engng. (ESCAPE-18). Chapter: Systematic Design of Production Processes for Enantiomers with Integration of Chromatography and Racemisation Reactions. 2008, p. 97–102.
- [153] J. C. Lagarias, J. A. Reeds, M. H. Wright, and P. E. Wright. Convergence Properties of the Nelder-Mead Simplex Method in Low Dimensions. *SIAM J Optimiz* 9 (1998) 112–147.
- [154] S. Golshan-Shirazi and G. Guiochon. Modeling of preparative liquid chromatography. *J Chromatogr A* 658 (1994) 149 – 171.
- [155] J. v. Langermann, Max Planck Institute, Magdeburg, Germany and M. Hedberg, AstraZeneca, Södertälje, Sweden. Personal communication (2011).
- [156] J.-E. Bäckvall, M. Hedberg, M. Kaspereit, A. Kienle, H. Lorenz, A. Seidel-Morgenstern, M. Shakeri, and J. von Langermann. Design of an Integrated Process for the Resolution of a Pharmaceutical Compound (working title). *Org Process Rev Dev* (in prep.).
- [157] M. Kaspereit, S. Swernath, J. G. Palacios, and A. Kienle. Evaluation of competing process concepts for the production of pure enantiomers. *Org Process Rev Dev* (in prep.).
- [158] C. A. Floudas. *Nonlinear and Mixed-Integer Optimization: Fundamentals and Applications*. Oxford University Press, New York, Oxford, 1995.
- [159] L. T. Biegler, I. E. Grossmann, and A. W. Westerberg. *Systematic Methods of Chemical Process Design*. Prentice Hall, 1997.
- [160] H. Yeomans and I. E. Grossmann. A systematic modeling framework of superstructure optimization in process synthesis. *Comp Chem Engng* 23 (1999) 709–731.
- [161] J. Gangadwala and A. Kienle. MINLP optimization of butyl acetate synthesis. *Chem Engng Proc* 46 (2007) 107–118.
- [162] Y. Kawajiri and L. T. Biegler. Nonlinear programming superstructure for optimal

- dynamic operations of simulated moving bed processes. *Ind Eng Chem Res* 45 (2006) 8503–8513.
- [163] Y. Kawajiri and L. T. Biegler. Optimization strategies for simulated moving bed and PowerFeed processes. *AIChE J* 52 (2006) 1343–1350.
- [164] T. Falk and A. Seidel-Morgenstern. Analysis of a discontinuously operated chromatographic reactor. *Chem Eng Sci* 57 (2002) 1599–1606.
- [165] T. Yun, G. Zhong, and G. Guiochon. Simulated moving bed under linear conditions: Experimental vs. calculated results. *AIChE J* 43 (1997) 935–945.
- [166] M. Kaspereit, J. G. Palacios, and D. F. und A. Kienle. Design of reactive and non-reactive simulated moving bed processes for Langmuir and bi-Langmuir isotherms using equilibrium theory (working title) (in prep.).
- [167] D. Flockerzi, A. Bohmann, and A. Kienle. On the existence and computation of reaction invariants. *Chem Eng Sci* 62 (2007) 4811 – 4816.
- [168] G. Severin. Spontaneous Racemization of Chlorthalidone: Kinetics and Activation Parameters. *Chirality* 4 (1992) 222–226.
- [169] E. Lamparter, G. Blaschke, and J. Schlüter. Racemization of Chlorthalidone in the Presence of Liposomes. *Chirality* 5 (1993) 370–374.
- [170] T. Borren and J. Fricke. In: H. Schmidt-Traub (Ed.): Preparative chromatography of fine chemical and pharmaceutical agents. Chapter: Chromatographic Reactors. Wiley-VCH, Weinheim, 2005.

## **Part II**

### **Enclosed Manuscripts**



## List of Enclosed Manuscripts

- PII-1 M. Kaspereit. In: E. Grushka and N. Grinberg (Eds.): *Advances in Chromatography*. Chapter: Advanced operating concepts for Simulated Moving Bed Processes. CRC Press, Taylor & Francis, Boca Raton/Fla, USA, 2009, 165–192.
- PII-2 T. Sainio and M. Kaspereit. Analysis of steady state recycling chromatography using equilibrium theory. *Sep Purif Technol* 66 (2009) 9–18.
- PII-3 M. Kaspereit and T. Sainio. Simplified Design of Steady-State Recycling Chromatography Under Ideal and Nonideal Conditions. *Chem Engng Sci* (2011, submitted).
- PII-4 P. Forssén, R. Arnell, M. Kaspereit, A. Seidel-Morgenstern, and T. Fornstedt. Effects of a Strongly Adsorbed Additive on Process Performance in Chiral Preparative Chromatography. *J Chromatogr A* 1212 (2008) 89–97.
- PII-5 M. Kaspereit, A. Seidel-Morgenstern, and A. Kienle. Design of Simulated Moving Bed Chromatography Under Reduced Purity Requirements. *J Chromatogr A* 1162 (2007) 2–13.
- PII-6 J. García Palacios, M. Kaspereit, G. Ziomek, D. Antos, and A. Seidel-Morgenstern. Optimization and Analysis of Possible Column Arrangements for Multicomponent Separations by Preparative Chromatography. *Ind Eng Chem Res* 48 (2009) 11.148–11.157.
- PII-7 J. Siitonen, T. Sainio, and M. Kaspereit. Theoretical analysis of steady state recycling chromatography with solvent removal. *Sep Purif Technol* 78 (2011) 21–32.
- PII-8 T. Sainio, M. Kaspereit, A. Kienle, and A. Seidel-Morgenstern. Thermal effects in reactive liquid chromatography. *Chem Engng Sci* 62 (2007) 5674–5681.
- PII-9 J. García Palacios, M. Kaspereit, and A. Kienle. Conceptual Design of Integrated Chromatographic Processes for the Production of Single (Stereo-)Isomers. *Chem Eng Technol* 32 (2009) 1392–1402.
- PII-10 J. García Palacios, M. Kaspereit, and A. Kienle. Integrated Simulated Moving Bed Processes for the Production of Single Enantiomers. *Chem Eng Technol* 34 (2011) 688–698.
- PII-11 J. García Palacios, B. Kramer, A. Kienle, and M. Kaspereit. Experimental Validation of a new Integrated Simulated Moving Bed Process for the Production of Single Enantiomers. *J Chromatogr A* 1218 (2011) 2232–2239.